TECHNO-ECONOMIC ASSESSMENT STUDY FOR ROGUN HYDROELECTRIC CONSTRUCTION PROJECT

PHASE II: PROJECT DEFINITIONS OPTIONS

Volume 2: Engineering and Design

Chapter 3: Design of alternatives

Appendix 2: Report on Embankment Dam Stability

August 2014

Report No. P.002378 RP 42 rev. C

C	14/08/2014	Final version – August 2014	OCL	LBO	LBO
B	31/03/2014	Final version – March 2014	OCL/EFD	NSA	NSA
A	08/04/2013	First Emission	OCL/CRO	RAC	NSA
Revision	**Date**	**Subject of revision**	**Drafted**	**Checked**	**Approved**

CONTENTS

FIGURES

TABLES

1 OBJECTIVES AND CONTEXT

This chapter addresses the technical assessment of Rogun dam stability. It includes a brief review of documents produced by HPI about the dam stability in 2009 and made available to the Consultant by the Client. It also includes the Consultant own assessment of the stability of the dam. It is to be noted that the Consultant chose to perform the stability analysis on the same typical cross section used in the calculation by HPI which matches the highest dam alternative (FSL 1290 masl).

The main objective of this study is to understand the dam behavior during earthquake and to evaluate the permanent displacement likely to occur during an extreme seismic event.

The results of this assessment are then used to derive the Consultant's own typical cross sections for the three different dam alternatives.

Once the most suitable alternative is selected, it is recommended to carry out further analysis considering all peculiarities of the dam, including 3D analysis.

2 REFERENCES

[1] S.L. Kramer, 1996. Geotechnical earthquake engineering, Prentice Hall.

[2] Newmark N.M, 1965. Effects of earthquake on dams and embankments, 5th Rankine lecture.

[3] F.I. Makdisi, H.B. Seed, 1978. Simplified procedure for estimating dam and embankment earthquake-induced deformations, Journal of the Geotechnical engineering division, ASCE.

[4] Swaisgood, 2003. Embankment dam deformations caused by earthquakes, Pacific conference on earthquake engineering, paper n°014.

[5] Dynamic modeling with QUAKE/W 2007, 2008, GEO-SLOPE International Ltd.

[6] Post, Tardieu, Lino, 1985. Conception parasismique des barrages, Génie parasismique VIII-1.

3 REVIEW OF HPI STUDY

The documents reviewed in order to understand previous studies in Rogun dam were the following:

Document N°	Document title - Russian	Document title - English	File
1	Оценка влияния растворения соли на устойчивость подземных выработок	Assessment of influence of dissolution of salt on stability of dam	3.pdf
2	Расчетное обоснование конструкций сооружений станции, плотины, водосбросных сооружений Расчетные исследования напряженно-деформированного состояния и устойчивости каменно-земляной плотины	Estimated study designs buildings stations, dams, water waste facilities calculations of the stress-strain state and the stability of the rock-earth dam (3d model).	4.pdf

	(пространственная задача).		
3	Расчетное обоснование конструкций сооружений станции, плотины, водосбросных сооружений Расчетные исследования напряженно-деформированного состояния и устойчивости каменно-земляной плотины (плоская задача).	Estimated study designs buildings stations, dams, water waste facilities Calculations of the stress-strain state and the stability rock-earth dam (plane problem).	5.pdf
4	Расчетное обоснование конструкций сооружений Станции плотины, водосбросных сооружений Оценка устойчивости откосов каменно - Земляной плотины	Computational basis of structures :Station dam, discharge structure Evaluation of rock slope stability earthen dam	8.pdf

Table 1: List of document reviewed

3.1 Stability analysis by static equilibrium

3.1.1 Description

The stability analyses are gathered in document No 4 (file 8.pdf). The reference stability criteria are given by Russian standard SNIP 33-01-2003 “Hydraulic Structures – Guidelines” According to this standard the relation between driving forces and resistant forces is given by:

$$\gamma_{lc} \cdot \gamma_n \leq \frac{R}{F}$$

where R and F are, respectively, the resultant for resistant and driving forces. The exact meaning of safety factor γ_n and γ_{lc} is not clear for the consultant.

In the present case $\gamma_n = 1.25$ and γ_{lc} varies from $\gamma_{lc} = 1.0$ for static analysis to $\gamma_{lc} = 0.85$ for seismic analysis. Therefore the security net factors are 1.25 for static stability and 1.065 for seismic stability.

The assessment of the overall safety factor is directly correlated to the mechanical parameters defined for the different zones in the dam. The documents reviewed provide the mechanical parameters given in the following table.

	Dam zone	ρ (t/m^3)	n	ρ (t/m^3)	ϕ (°)	C (MPa)	E (MPa)	ν	K (cm/s)
1	Core	2.36	0.19	1.39	31	0.03	40	0.36	A*10-6
2	Fine transition	2.21	0.22	1.32	36	0.0	55	0.32	3*10-2
3	Coarse transition	2.26	0.20	1.35	40	0.0	65	0.30	5*10-2
4	Rockfill	1.99	0.30	1.19	42	0.03	60	0.28	0.50
5	Gravel	2.31	0.18	1.38	39	0.05	80	0.27	0.10

Table 2: Mechanical parameters for soils in stability analyses

The stability analysis report is divided into three parts, the first part concerns the stability of the upstream cofferdam, the second part is dedicated to the stage 1 dam, and the third part to the stability of the stage 2. Some generalities of these analyses are presented hereafter.

Upstream cofferdam: The main objective in this stage concerned the stability study of the upstream slope regarding two design options. The first option included an upstream impervious core, and the second option an impervious membrane. In both cases both static and seismic security factors were above the limit criteria.

Stage 1 stability analysis: the main works showed in this section concerned the optimization of the section (downstream slope and maximal height) of the stage 1 dam. Four different options were analyzed, three of them keeping a crest height at 1100 level and changing downstream slope, and the fourth one with a lower crest height (1060). From this study it was concluded that downstream slope should be greater than 1v-1.68h to fulfill stability criteria for both static and dynamic conditions.

Stage 2 stability analysis: In this section two seismic magnitudes (8 and 9 points) were imposed to three different sections of the dam and including two variations concerning a zone with coarse rockfill. Stability criteria in maximum section are fulfilled for both options in static conditions and in seismic loading of 8 points (both up and downstream). However, seismic criterion is not fulfilled for 9 points earthquake. Therefore, in order to fulfill also the 9 points earthquake horizontal reinforcement at different levels is proposed.

3.1.2 Comments

For static stability the overall safety factor given by Russian guideline is, 1.25 for static stability and 1.065 for seismic stability, ie below the limit criteria given by the TEAS design criteria (USBR recommendation) which is equal to 1.5 for long-term stability.

The hypothesis taken about the materials mechanical properties are consistent with the materials specifications (see Geotechnical report);

The seismic load cases are not detailed, it is not said what is exactly the additional gravitational forces taken into account in the pseudo static analysis.

The reinforcement proposed here is not retained by HPI given the results of the more detailed calculation performed (see next §).

3.2 Static analysis with 2D finite element model

3.2.1 Description

The finite element (FE) analyses were developed in order to assess an order of magnitude of displacements and stresses in the structure during construction and operation conditions.

The first study concerns the strain-stress behavior of the highest section of the dam. A 2D model is developed in report N°3 (see Table 1). In this report the construction phasing (static analysis) was modeled in order to estimate the settlements and the stress state at the end of construction.

The construction of the dam was modeled by activation of horizontal layers. The maximum settlement was estimated to 5.6 m in the core of the dam between levels 1050 and 1070 masl. The maximum vertical stress reaches 1117 t/m² near the upstream toe of the core.

The vertical stress and the water pressure obtained from the static analysis are shown in Figure 5.1.

3.2.2 Comments

The analysis performed seems to be non-linear: it takes into account the elastic and plastic behavior of the soil.

The model defined and employed in reports N°2 and 3 requires the definition of several parameters, in order to define the elastic characteristics, the shear envelope, the hardening functions and the initial elastic domain. However on reports N°2 and 3 only elastic characteristics and shear envelope parameters are defined (i.e. only 4 parameters over 10). Therefore it is not possible to verify if the set of parameters adopted are representative of the mechanical behavior observed in laboratory tests.

The total vertical stress and pore water pressure calculated at the end of the reservoir impounding are reproduced in

Figure 3.1. It shows some features that are not understood by the Consultant:

1. Pore pressure distribution is not consistent with the load case: variation of pore water pressure is expected in the upstream dam shell and not only in the core.

2. the stress distribution along the transition zones around the core : normally it is expected a contrast in stress distribution due to the difference in deformation modulus between two adjacent materials. Nevertheless, here the variation observed is very important. It is remarked that the vertical stress falls lower than 1.3MPa to 300m depth (for reference geostatic stress would be higher than 7MPa).

The Consultant has a partial understanding of HPI calculations made available. Therefore, it was found necessary to carry out independent calculations. The maximal section was analyzed under static conditions after impounding. In order to make both simulations (HPI and TEAS) equivalent, the same mechanical parameters defined in document 3 (see Table 1) were used. The results in terms of effective vertical stresses are shown in

Figure 3.2. It shows that the maximum vertical effective stress at the upstream toe of the core is roughly superior to 3.0 MPa.

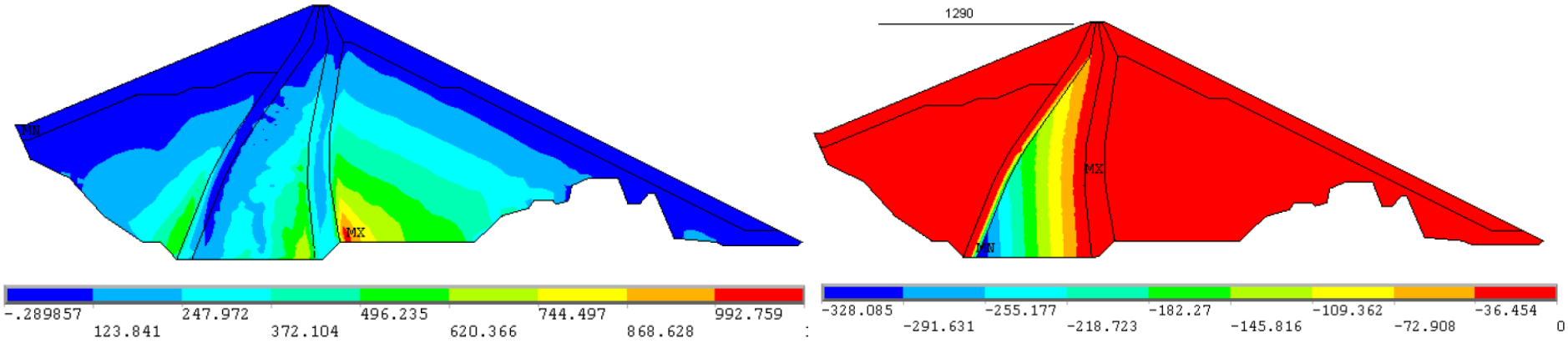

a) Vertical stress Sz (t/m²) on the maximum section of the dam

b) Water pore pressure (t/m²)

Figure 3.1 : HPI results - 2D finite element modelisation

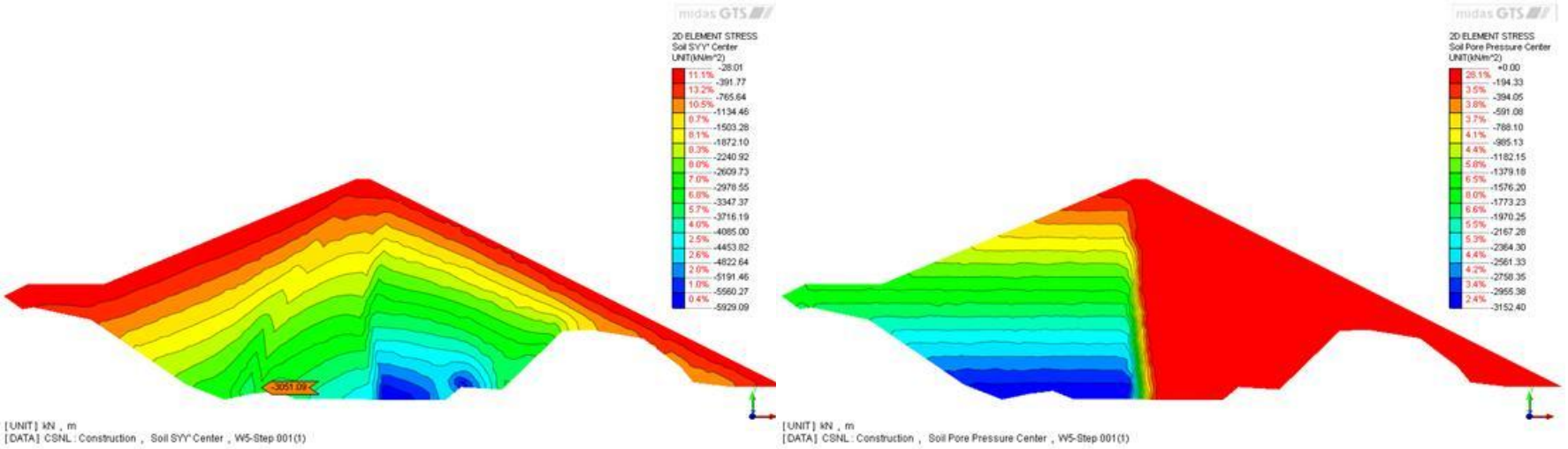

a) Vertical effective stress Sz (kPa) on the maximum section of the dam (Compression is negative)

b) Water pore pressure (kPa)

Figure 3.2 : TEAS results – Static condition after impounding

3.3 Dynamic analysis with 2D finite element modeling

3.3.1 Description

In this section the objective is to evaluate the level of stresses and displacements induced by earthquakes.

The natural period of the cross section was estimated to 3s.

The dynamic analysis consisted on 10 time history analysis, i.e., the acceleration at the base of the model is imposed by a signal. All the acceleration records had a peak acceleration of 5.4 m/s², ie 0.55 g. The displacements generated by the 10 cases are resumed in Table 3.

N	Maximum displacement, m		Maximum residual displacement, m		Crest settlement, m
	Horizontal	Vertical	Horizontal	Vertical	
1	0.12	0.30	0.12	0.13	0.08
2	0.18	0.22	0.12	0.15	0.05
3	0.59	0.79	0.49	0.55	0.30
4	0.08	0.13	0.07	0.08	0.02
5	0.30	0.33	0.28	0.23	0.05
6	0.29	0.11	0.11	0.10	0.04
7	0.93	0.83	0.61	0.59	0.51
8	0.10	0.10	0.06	0.05	0.03
9	0.13	0.15	0.09	0.10	0.06
10	0.43	0.58	0.11	0.3	

Table 3: Results from HPI 2D dynamic analyses

3.3.2 Comments

The first stage in a dynamic analysis consists in defining the initial stress state in the media, which is obtained from the previous static analysis. Therefore the response of the dynamic analysis is linked strongly to the results of the static study.

As in the 2D FE static study the material characteristics are not presented.

The earthquakes considered have all a PGA of 0.55 g which is below the MCE considered by the TEAS Consultant.

The results showed a dam first natural period of 3 s which is high. The matching shear velocity is 290 m/s and gives a dynamic shear modulus of 182 MPa.

3.4 3D finite element analysis

3.4.1 Description

This study concerns the strain-stress behavior of the entire dam – report N°2, file 4.pdf. A 3D model has been developed following the same procedure as for the 2D case.

The construction of the dam was modeled by activation of horizontal layers. The maximum settlement was estimated to 4.4m, against 5.6m for the 2D model. The maximum vertical stress reaches 978 t/m², against 1117 t/m² for the 2D model.

For 3D model the natural period of oscillation was estimated to 2s (against 3s for the 2D analysis). For 3D model only the most critical earthquake was applied to the model. As in the previous 2D case the peak acceleration was of 5.4 m²/s, ie 0.55 g.

Peak acceleration at crest induced by the earthquake was estimated to 8.2 m/s², ie 0.84 g.

3.4.2 Comments

Comparison between the 3D and 2D analysis shows that 3D effect reduces the effective vertical stress on the dam's core.

As in the 2D static study the material characteristics are not presented in the reports made available to the Consultant.

Broadly speaking the same remarks made as before are valid for this analysis. For instance, as seen in Figure 3.3, the vertical stress at the highest section shows also an unexpected low value at the contact between the filters and the core.

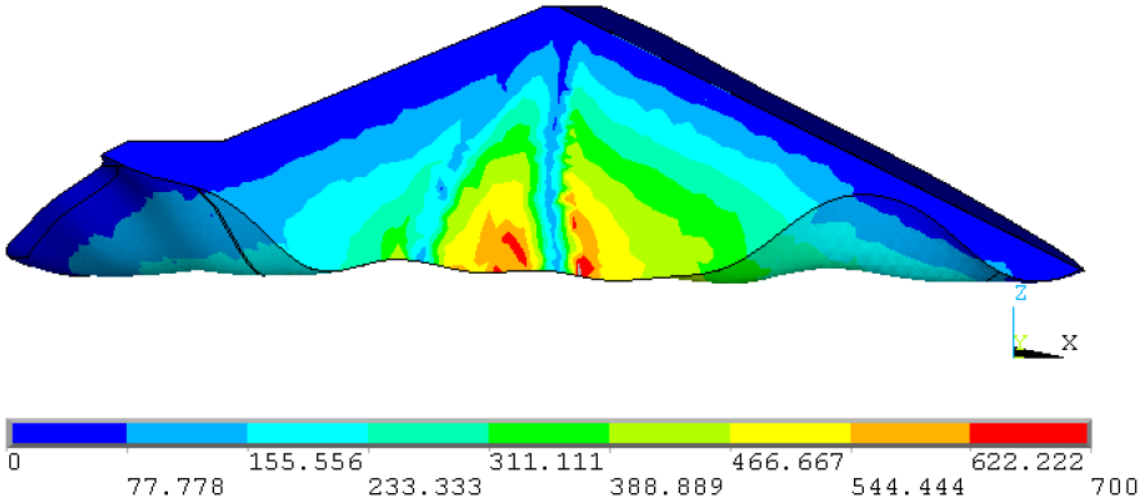

Рис. 4.19 Вертикальные напряжения Sz(т/м^2) в поперечном сечении плотины

Figure 3.3: HPI 3D static study results

3.5 Synthesis

In general, the review of the documents made available to the Consultant shows that many elements of the HPI analysis, especially the material dynamic properties, are unclear.

Nevertheless, it is to be noted that:

- The stability analysis by static equilibrium showed that the dam stability in static conditions is ensured;
- The results of the static analysis with the 2D finite element model are unclear but the check calculation made by the Consultant showed acceptable results;
- The level of seismic loading considered by HPI (PGA of 0.55g) is lower than the one recommended by the Consultant (PGA of 0.71g);

All of the above lead the Consultant to make its own independent assessment of the dam stability.

4 SCOPE OF THE PRESENT STUDY

The Consultant performed independent calculation of the dam in the scope of its technical assessment of HPI study. It aimed at appreciating the dam safety in static and seismic condition.

4.1 Static analysis

Stability of slopes generally are assessed thanks to limit equilibrium analysis of a potential sliding mass discretized into vertical slices

Many different solutions for the method of slices have been developed over the years and the differences between all of them are mainly due the assumptions on inter-slices forces.

The Consultant carried on a slope stability analysis with the Morgenstern and Price method which satisfies equilibrium equations in introducing slice forces. The Consultant understands that HPI carried out its calculations with a method that could be similar to the Fellenius method (which is not introducing lateral slice forces). The critical safety factor found with the Fellenius method is lower than the one found with Morgensten & Price as the assumptions are safer but farther from reality.

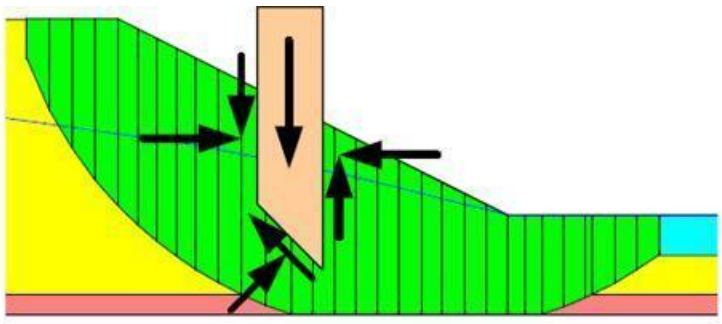

Figure 4.1: Slice discretization and slice forces in a sliding mass

The static analysis is presented in paragraph 5.

4.2 Seismic analysis

The analysis of the dam behavior during an earthquake is a complicated question that has led to the creation of various methods over the years.

First, some empirical method exists, like Bureau (1985) or, Swaisgood (2005), that implemented some correlation between the maximum settlement due to an earthquake given its characteristics.

Then there are the analytical methods. The behavior of an embankment dam during a seismic event is complex and includes several specific aspects:

- The seismic additional gravitational constrains;
- the embankment elastic response to dynamic excitement that depends on its geometry and stiffness;
- the cyclical stresses generated during an earthquake that can influence the mechanical characteristics of the material.
- The plastic deformation of the materials;

All those aspects are important, but can not be taken into account all together in a simple method. Therefore, several simplified method have been implemented.

The pseudo-static method is the first analytical solution imagined to evaluate the stability of a dam during an earthquake. It considered the seismic load as a constant additional horizontal or vertical inertial force. This method is very simplistic and does not take into account any dynamic behavior (elastic response, irreversible movement…).

Newmark (1965) was the first one to develop a pseudo-dynamic method to assess the possible irreversible movement. Based on the pseudo-static calculation, the critical acceleration (yield acceleration) that respects a safety factor of 1 was found and a double integration of the

accelerogram gives a cumulative irreversible movement of the slipping mass that could happen during the earthquake.

Several authors proposed simplified method that, in addition to Newmark method, takes into account the vibratory behavior of the dam: Ambraseys and Sarma (1967), Makdisi and Seed (1978), Ambraseys and Menu (1988)… All those method assume small irreversible displacements.

A numerical model is a powerful tool that can help the analysis by modeling all or some of the nonlinear behavior of the dam.

In the case of Rogun, and at his stage of the study, five different 2D methods are used (see §6):

- A pseudo static approach to assess the sensitivity of the structure to an additional load;
- Swaisgood: this empirical method gives a maximum crest settlement;
- A finite element modelisation: with first a linear elastic and then a linear equivalent calculation;
- Makdisi and Seed : a simplified analytical method that gives a maximum irreversible deformation;
- Newmark method that also gives the maximum irreversible deformation based on the finite element modelisaton resutls.

Those three methods will allow reasonable assessment the dam behavior during seismic event.

It is certain that the 3D effect of the Rogun narrow valley is important and a 3D calculation will be necessary in further stages of the studies.

4.3 Stage 1 stability

An independent analysis have been performed for the Stage 1 which is presented in §7.

4.4 Foundation conditions

The foundation conditions are addressed in the geotechnical report and the conclusions are repeated here: they do not consider failure surfaces likely to affect some part of the foundation.

As the possibility of some erosion potential has been detected, it has been addressed by specific mitigation measures (extension of impervious grout curtain aimed at lengthening the potential underground waterflow lines, in order to limit the hydraulic gradients).

In order to keep control on the risks associated with temporary slope stability problems during construction, significant preparatory site works will have to be devoted first, to secure the construction site slopes against loose unstable rocks, risks of rock fall, etc., and second, during the construction, particular care and caution will be devoted to this aspect of the works.

5 STATIC ANALYSIS PERFORMED BY THE CONSULTANT

5.1 Design criteria and load cases

The stability verification on static load cases are required to verify the design criteria recommended by the USBR in its Design Standards n°13-Chap4.

For each loading condition, the critical safety factor found shall be equal or higher than the minimum safety factor allowed.

	Loading condition	Minimum safety factor
1	End of construction	1.3
2	Normal condition - Water level at FSL	1.5
3	Normal condition – Water level at MOL	1.5
4	Rapid drawdown from FSL to MOL	1.3

Table 4 : Design criteria

The loading condition 1 “end of construction” describes the situation when the dam is completed and the reservoir is empty. The pore pressures in the dam are defined thanks to the Ru coefficient. This load case does not really exist for the Rogun dam as it is filled while constructed, but it is study as a reference case.

5.2 Geometry

The geometry used in the static stability analysis is several cross-section of the design study by HPI in their 2009 calculation notes. The typical cross section is presented in the next figure.

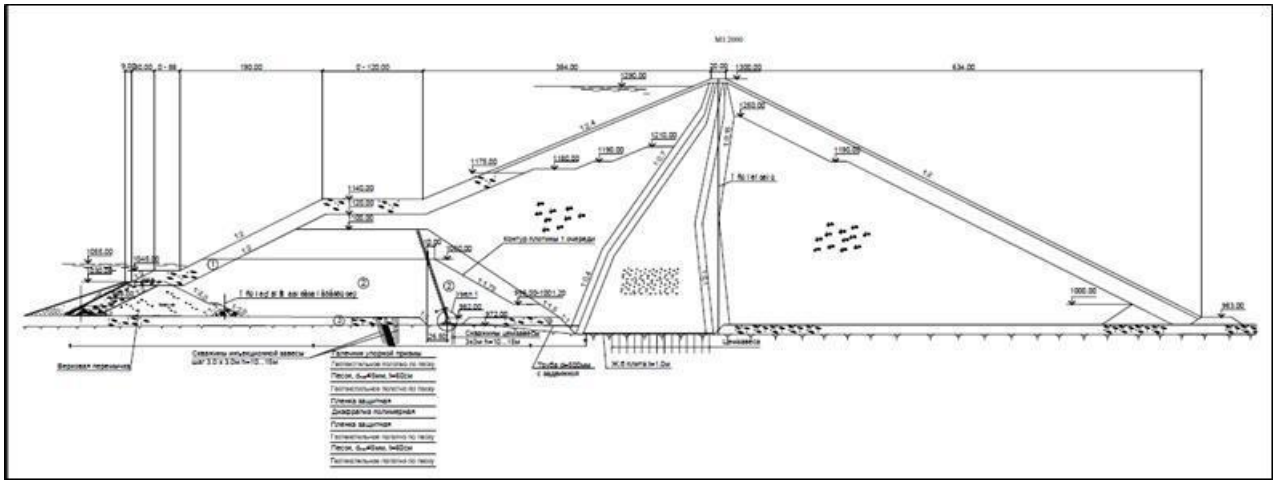

Figure 5.1: Calculation cross section (extract from “Dam stability 3D modelling, Hydroproject, 2009)

As the valley is S-shaped, the typical cross section as presented in the previous figure is not a real cross section. Therefore, several “real” cross sections are studied. They are indicated on the next figure.

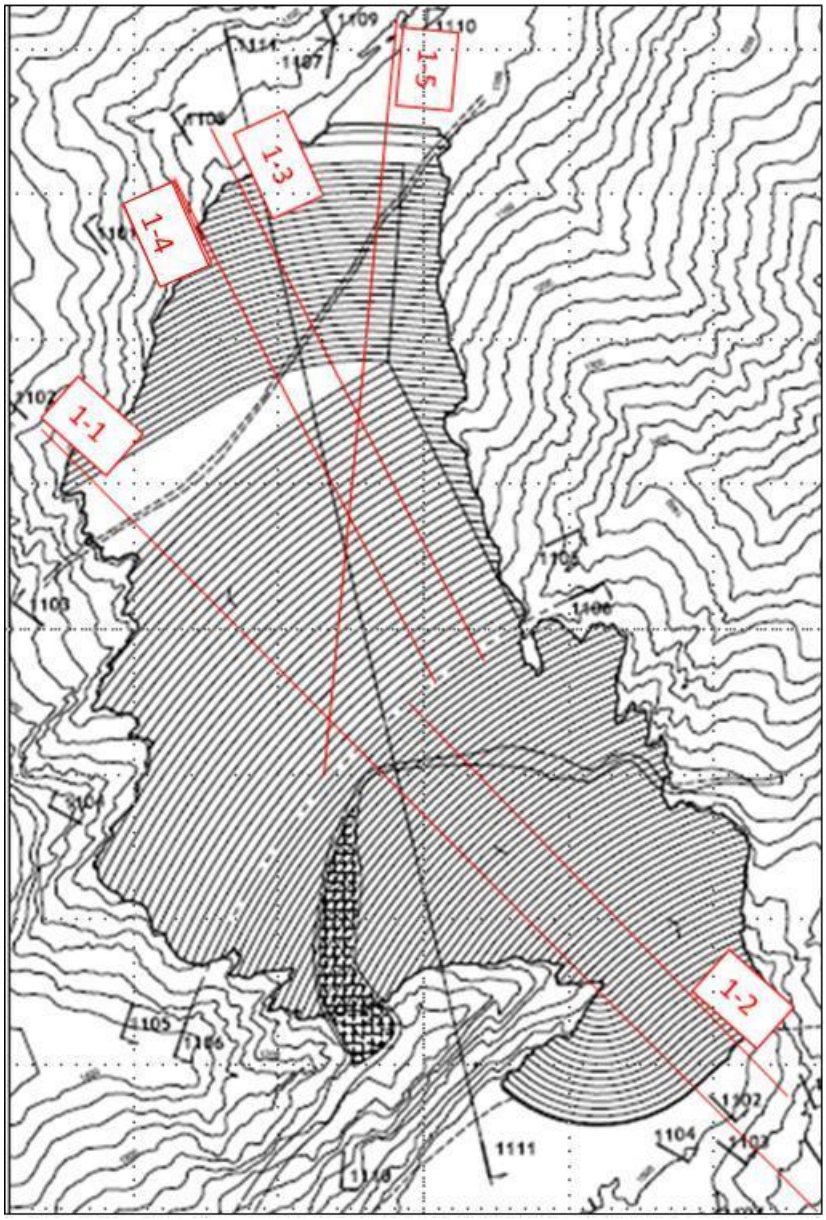

Figure 5.2 : Layout of the cross-sections

Cross section 1-1 is the one studied by HPI. Cross section 1-2 presents a full downstream slope: full height and full length. Cross-sections 1-3 and 1-4 are the full upstream slope with a two different width for the risberm. And cross section 1-5 is normal to the stage 1 slope. This one aims at assess the safety factor of the Stage 1slope that is stiffer than the general upstream slope of the dam (1:2 for the Stage 1 and 1:2.4 for the dam).

5.3 Material properties

The material properties considered in the study are the same as the one used by HPI studies, as they were considered representative of the material conditions.

	C' (MPa)	φ' (°)	γ (kN/m^3)	γ_{sat} (kN/m^3)	Ru
Core	0.03	31	23.6	23.9	0.5
Fine filter	0	36	22.1	23.2	0
Coarse filter	0	40	22.6	23.5	0
Gravel shells	0.05	39	23.1	23.8	0
Rockfill	0.03	42	19.9	21.9	0

Table 5 : Static analysis - material properties

5.3.1 Comment on the shear strength

Rockfill embankments exhibit usually non-linear strength envelope, as significant developments on the subject have been made in our company (*1*).

However, the effective determination of non-linear shear strength envelope for a given rockfill requires a heavy effort in testing, either in terms of costs or time, because of the uncommon size of samples and apparatuses to be handled. These are the main reasons why such effective measurements of this non-linear strength envelope are only seldom performed (*2*).

In the specific situation of Rogun Project, the data base from HPI allowed to review the proposed parameters, but not to perform a full re-interpretation of performed test data within the present studies time-frame.

The physical meaning of shear strength parameters shall be understood as related to the way they are used to schematize a non-linear shear strength envelope, as shown in the following Figure 5.3.

1 Ref. for instance E. Frossard: *« Granular Materials in Civil Engineering : Recent Advances in the Physics of their mechanical Behaviour and Applications to Engineering» in* Multiscale Geomechanics– *Collective book,* Dir. P.Y Hicher, ISTE Ltd - J.Wiley & Sons publishers, London(UK), Hoboken(USA), Jan 2012, p.35 – 81, ISBN 978-1-84821-246-6, or E. Frossard & al. « *Rockfill shear strength evaluation: a rational method based on size effects* » Géotechnique 62, No5, 415-427, London, May 2012.

2 *Ref. J. Michael Duncan* « Friction Angles for Sand, Gravel, and Rockfill » *Notes of a Lecture presented at Kenneth L. Lee Memorial Seminar, Long Beach- California, 28 Apr. 2004*

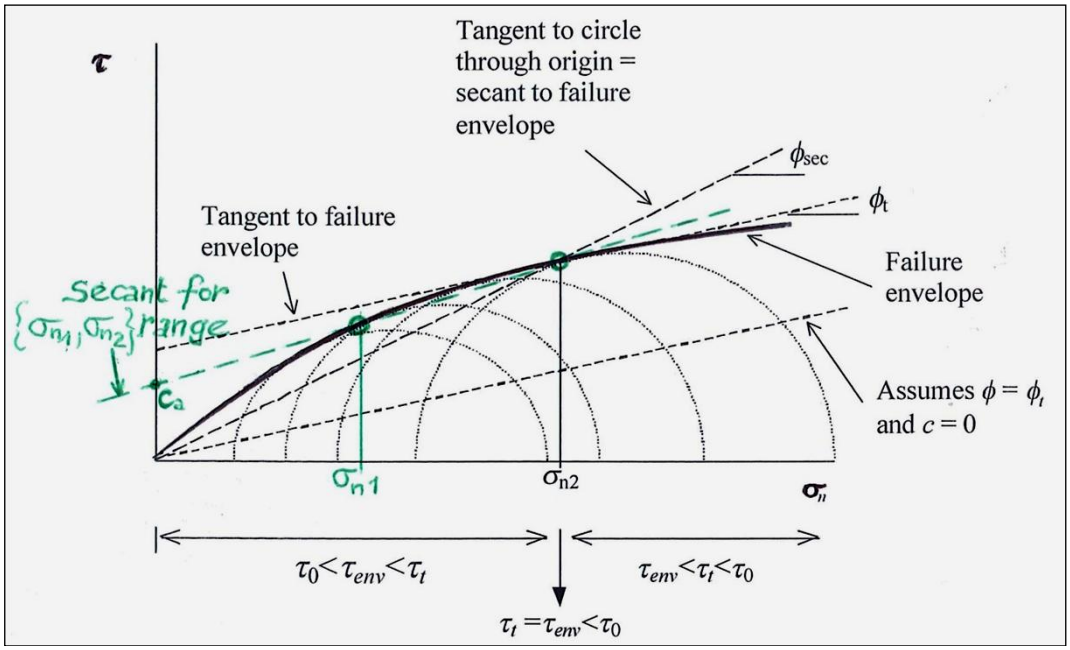

Figure 5.3 : Representations of a non-linear shear strength envelope

When a straight line, with 2 parameters "apparent" cohesion C_a and "apparent" internal friction φ_a, is used to represent the non-linear shear strength envelope of a rockfill over a certain range of normal stresses (see "Secant for $\{\sigma_{n1}, \sigma_{n2}\}$ range" on Figure 5.3), the corresponding "apparent" cohesion C_a has not the same physical meaning as if a truly cohesive clayey material were considered. It shall be considered better as a mere parameter, provided both parameters C_a and φ_a are used reasonably to represent the shear resistance of rockfill in the specific range of normal stresses.

To check that these "apparent" cohesions and internal frictions assumed for Rogun materials do reasonably correspond to the range of shear resistance data of rockfills and gravels, these have been compared with relevant data:

- In the usual diagram $\{ \tau \ \sigma_n \}$ on following Figure 5.4, with central trend fitted to large size triaxial tests data compiled by Charles & Watts (1980) (*3*), which may be represented for materials D_{Max} 150mm, by $\tau = 3{,}6.\sigma_n^{0.8}$ (in kPa), and central trend for large shear box test data which may be represented for materials D_{Max} 150mm, by $\tau = 5{,}5.\ \sigma_n^{0.75}$ (in kPa);

- In the diagram $\{\varphi_{secant}\ ,\ \sigma_n\}$ on following Figure 5.5, together with the central trends displayed on Figure 5.4, and the data of 226 large triaxial tests gathered by Woodward-Clyde company in a work for the very large Diamond Reservoir Project in Southern California, and reproduced in the above mentioned ref 2 (J.M. Duncan-2004); note that in such a diagram, the straight lines for rockfill and gravel do transform into curved lines in Figure 5.5, because of the definition of φ_{secant}.

On these Figure 5.4 and Figure 5.5, the shear strengths assumed for Rogun materials Rockfill (green line, with C_a =30 kPa φ_a=42°) and Gravel (violet line with C_a =50 KPa φ_a =39°) are laying

3 *Charles J.A. Watts K.S.* "The influence of confining pressure on the shear strength of compacted rockfill" *Géotechnique 30, (4) 353-367, London, 1980*

quite well in the core data range for normal stresses below 1800 kPa (or 170 PSI), and appear somewhat on the upper range for normal stresses above 1800 kPa.

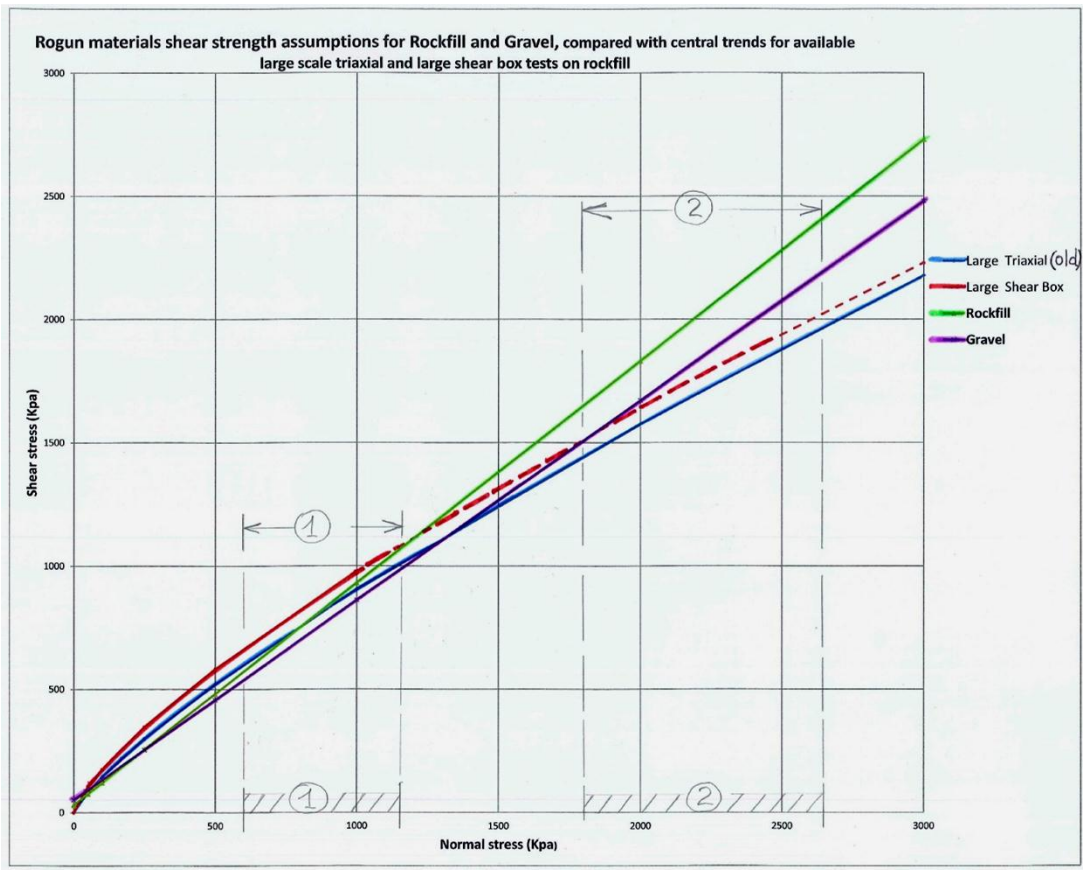

Figure 5.4

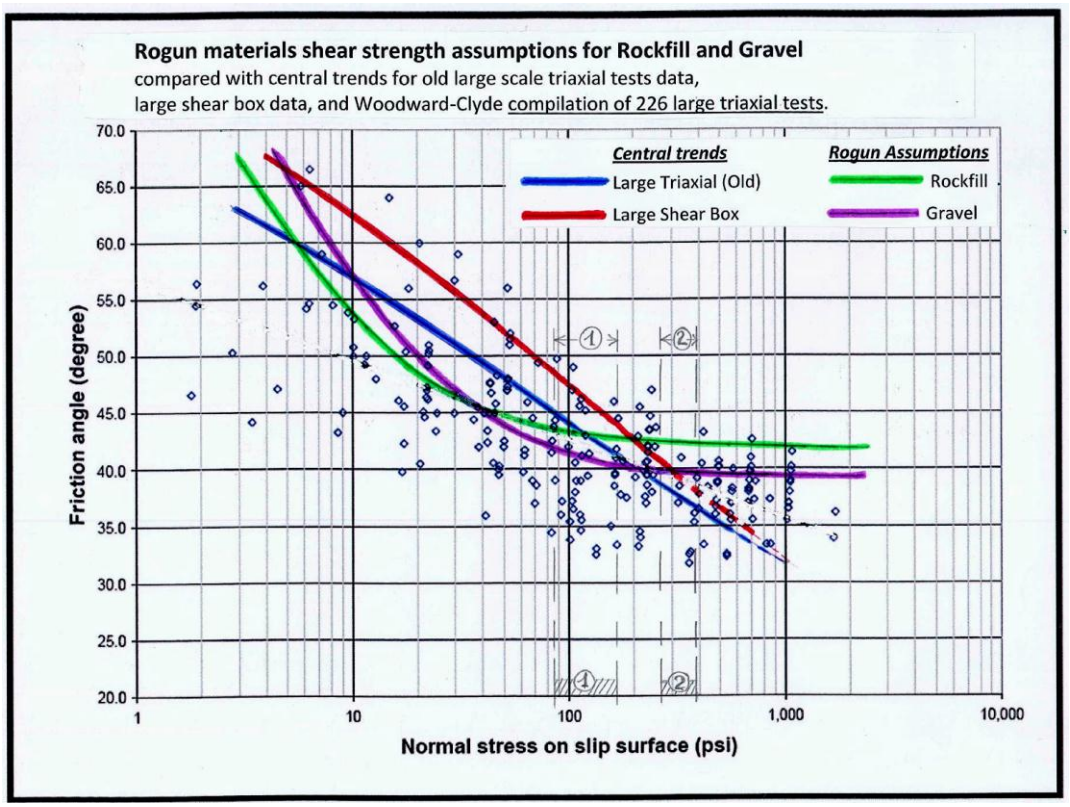

Figure 5.5

In Figure 5.5, it appears also that should an assumption C_a=0 to be made into Rockfill and Gravel simplified strength formulation, it would transform the corresponding green and violet curves into horizontal straight lines for φ_{secant} 42° and 38°. Compared with the data, this situation would result quite over-conservative for normal stresses lower than about 150 Psi, or 1 MPa.

The relevance of these shear strength assumptions regarding usual shear strength data being addressed, the remaining question is then the relevance of these shear strength assumptions for the range of normal stresses computed in the stability analysis.

This is the subject of the back analysis presented in the paragraph 5.5.

5.3.2 Comment on of Ru

The value assumed in our analysis Ru=0,5 has been chosen from our experience, on the conservative side.

Reference values may be found in back-analysis of relevant large dams built in the past:

- **Oroville Dam** (234m in height, 60 millions cum. materials, end of construction 1967, California) - This landmark in the history of dams is especially interesting because of its core slightly inclined towards upstream, with a constitution similar to the Rogun core. The dam was well instrumented, and computations by finite elements method have been performed

after the end of construction by F.H. Kulhawy and J.M. Duncan (*4*); the pore pressure was computed on the base of a coefficient of 0,5, by two approaches:

- On the base of major principal stress σ1 equal to γh (in this situation $\overline{B}$ = Ru)
- On the base of major principal stress σ 1 given by finite elements computations

The comparison of measured pore pressures at end of construction with the values computed led to the conclusion that the coefficient $\overline{B}$ (and also the Ru) actual is significantly lower than the assumed 0,5: although variable within the core, its value do not exceed 0,3.

Of course, the value of Ru in the core depends on the speed of raising of the dam earthfill works. In the case of Oroville, the dam was built in 7 years, (about 35m per year), which is consistent with what is expected for Rogun.

- **Mica Dam** (244m in height, end of construction 1973, Canada) This is another large dam with a core similar to Rogun one, except that Mica Dam core is constituted of moraine instead of alluvium, for which a confrontation between measurements and computations is available (*5*). The pore pressures measured at the end of construction correspond to a Ru between 0,15 and 0,35, then quite below 0,5.

- It should be very interesting to have the same kind of analysis performed for Nurek Dam.

In a review of the methods available for prediction of pore pressures (*6*) in stability analysis, D.G. Fredlund states as follows:

" ..There is no theory available to predict the pore pressure coefficient. Rather the value for the pore pressure coefficient is assumed, based on experiments. Design values generally range from 0,3 to 0,45. Experience has shown that problems with instability generally occur when the pore pressure coefficient exceeds approximately 0,35…"

Two relevant specificities of Rogun Dam Project shall be also recalled:

- Rogun core material will be constituted by a large proportion of gravels and cobbles in order to limit the compressibility, and so the settlements; this will also contribute to limit the rise of pore pressures at end of construction, in comparison with a common clay core material, as a significant part of the vertical loads will be supported by the granular phase within the core material;

- Rogun dam site configuration is strongly three-dimensional, not only because of its narrowness (ratio width / height, or L/H, less than 2) but also because of its tortuosity (the site is quite curved in a plan view), these features will participate in restraining the settlements, as in such configurations vertical loads are partly transferred to the abutments instead of transmitting fully vertically down to the toe of dam core.

4 *Kulhawy F.H., Duncan J.M.* "Stresses and movements in Oroville Dam » *ASCE Journal of Soil Mech. & Found. Div. Vol 98, N° SM7, 653-665, April 1973*

5 *Eisenstein Z., Law S.T.* « Analysis of consolidation behavior of Mica Dam » *ASCE Journal of the Geotechnical Enging. Div. Vol 103, N° 8 August 1977, 879-895, Aug. 1977*

6 *Fredlund D.G., Barbour S.L.*« The prediction of pore pressures for slope stability analysis » *Slope stability Seminar, University of Saskatchewan, April 1986*

So, for what precedes, the assumption Ru= 0,5 for Rogun core material appears to be a quite reasonable value, even a pessimistic one, given the relevant particularities of Rogun Dam Project outlined above.

5.4 Results

The next table the minimum safety factors that have been found for all calculation made: all loading conditions, and all cross sections. The sign – means that this calculation is not available because this load condition on this cross section has no meaning.

	Loading condition	Slope	1-1	1-2	1-3	1-4	1-5	HPI results
1	End of construction	Upstream	2.37	-	2.26	2.39	2.00	-
		Downstream	1.87	1.85	-	-	-	-
2	Normal condition - Water level at FSL	Upstream	2.54	-	2.37	2.49	1.94	2.06
		Downstream	1.87	1.84	-	-	-	1.64
3	Normal condition – Water level at MOL	Upstream	2.16	-	2.12	2.15	2.18	-
4	Rapid drawdown from FSL to MOL	Upstream	2.08	-	2.02	2.14		-

Table 6 : Static analysis – Results

For all loading condition, the static design criteria are respected. HPI results are lower, which can be explained by the calculation method that is different : Fellenius vs Morgenstern-Price.

The next figures show the critical slip surface for each cross section and loading conditions.

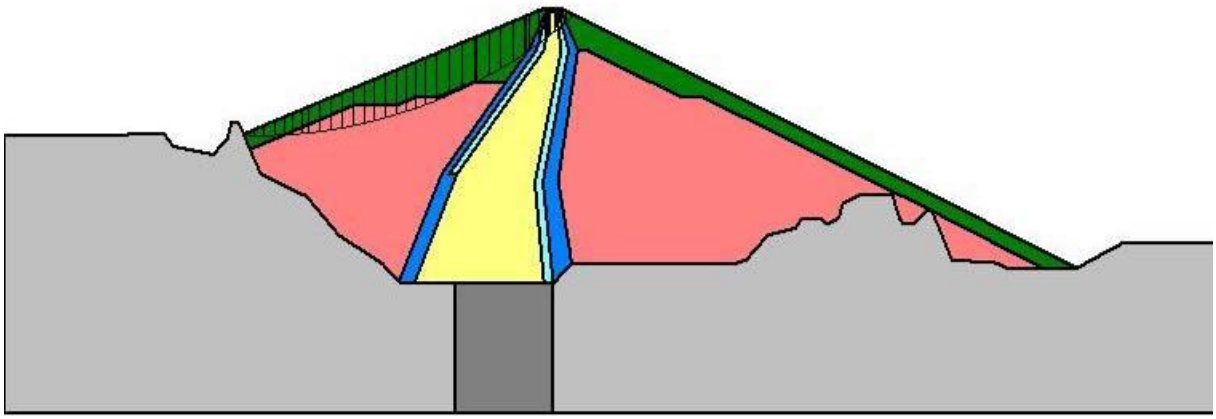

Figure 5.6 : Critical slip circle - Load case 1 - Cross section 1-1 upstream (FS=2.37)

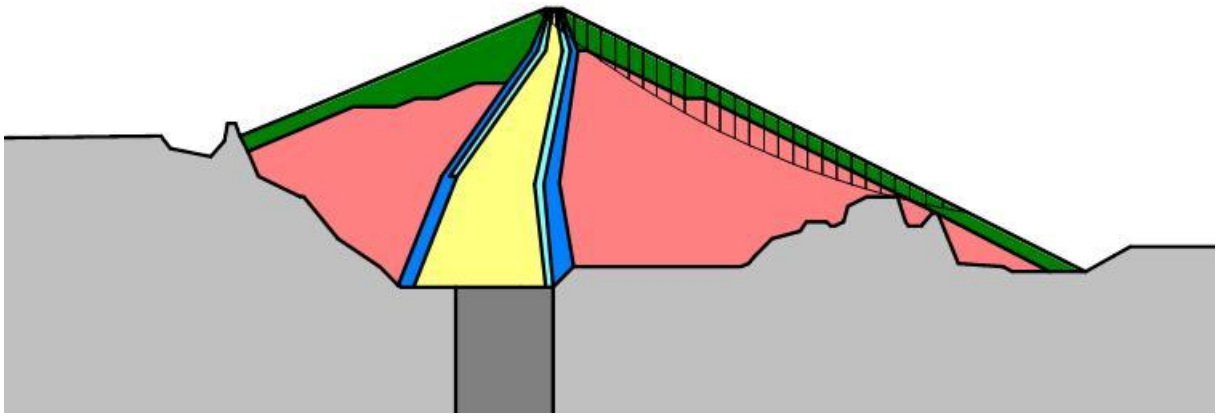

Figure 5.7 : Critical slip circle - Load case 1 - Cross section 1-1 downstream (FS=1.87)

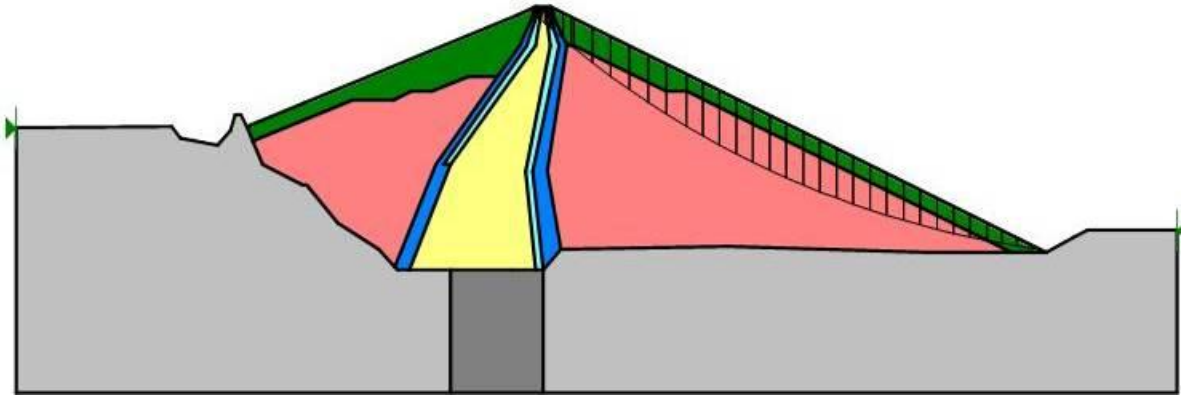

Figure 5.8 : Critical slip circle - Load case 1 - Cross section 1-2 downstream (FS=1.85)

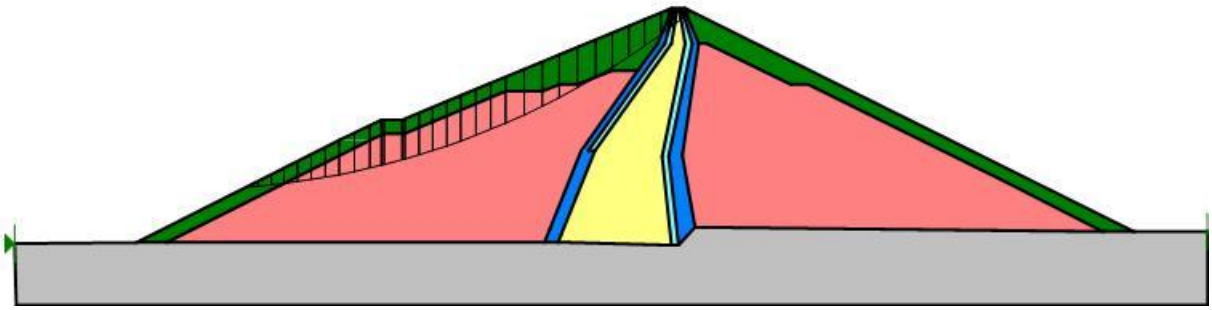

Figure 5.9 : Critical slip circle - Load case 1 - Cross section 1-3 upstream (FS=2.26)

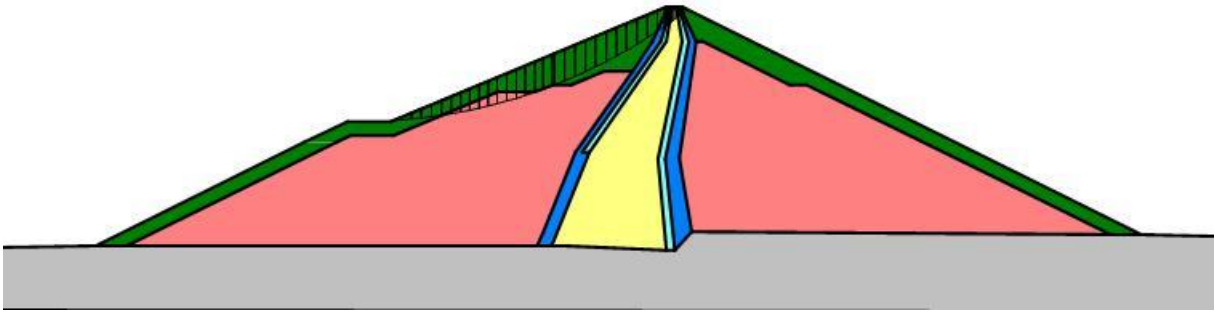

Figure 5.10 : Critical slip circle - Load case 1 - Cross section 1-4 upstream (FS=2.39)

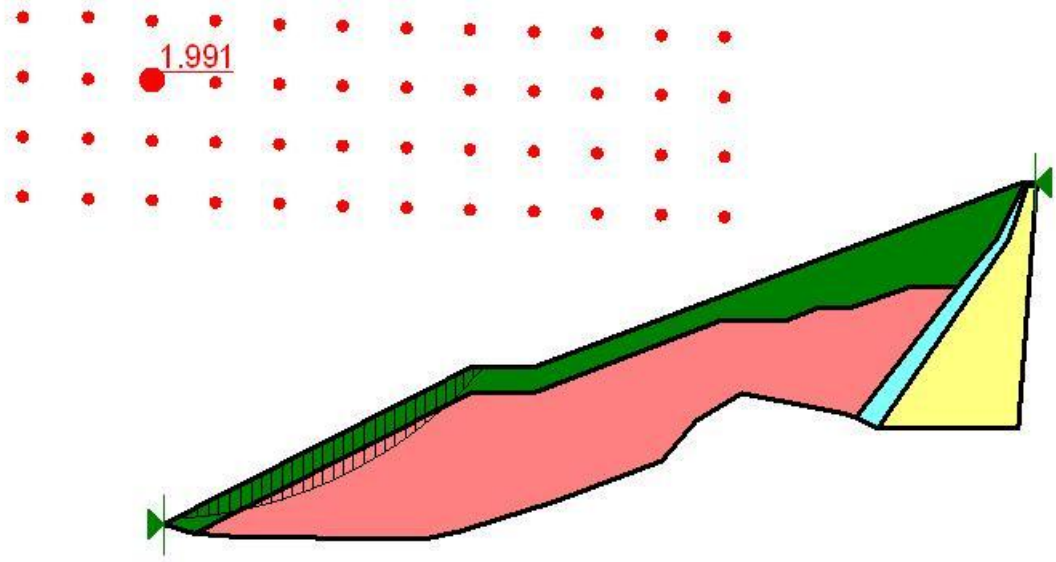

Figure 5.11 : Critical slip circle - Load case 1 - Cross section 1-5 upstream (FS=1.99)

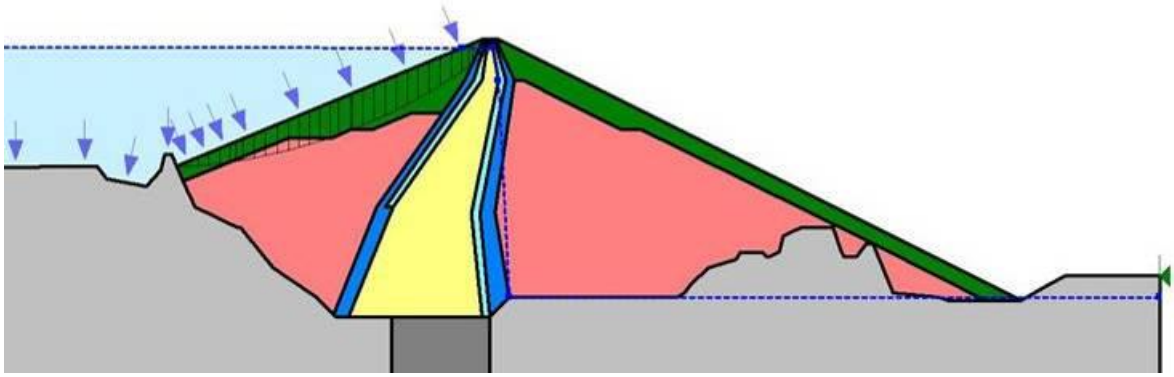

Figure 5.12 : Critical slip circle - Load case 2 - Cross section 1-1 upstream (FS=2.54)

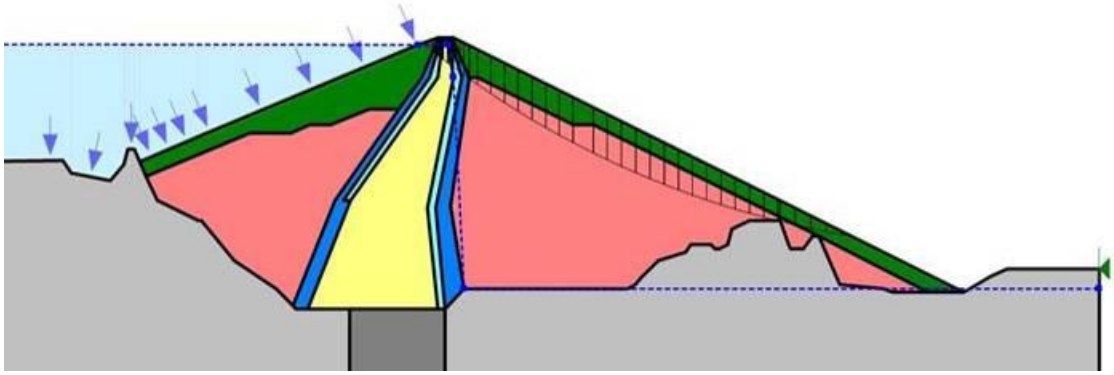

Figure 5.13 : Critical slip circle - Load case 2 - Cross section 1-1 downstream (FS=1.87)

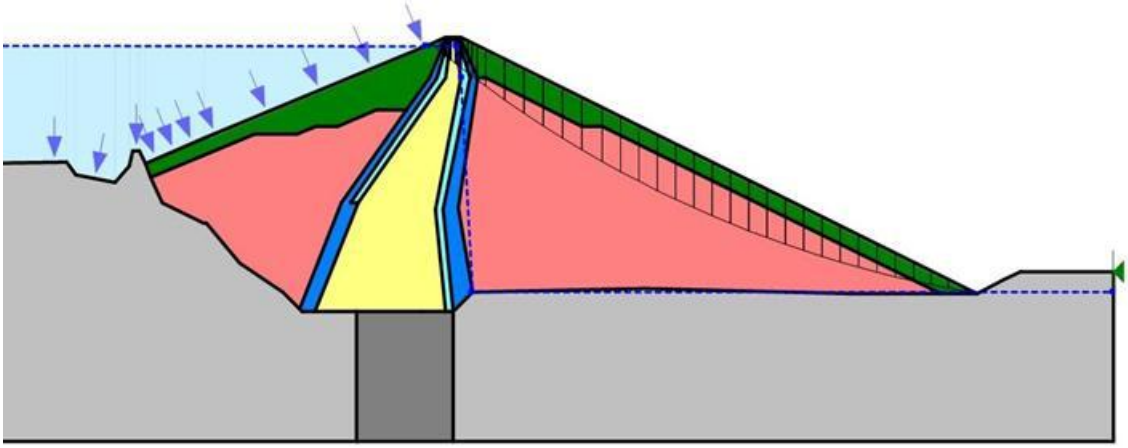

Figure 5.14 : Critical slip circle - Load case 2 - Cross section 1-2 downstream (FS=1.84)

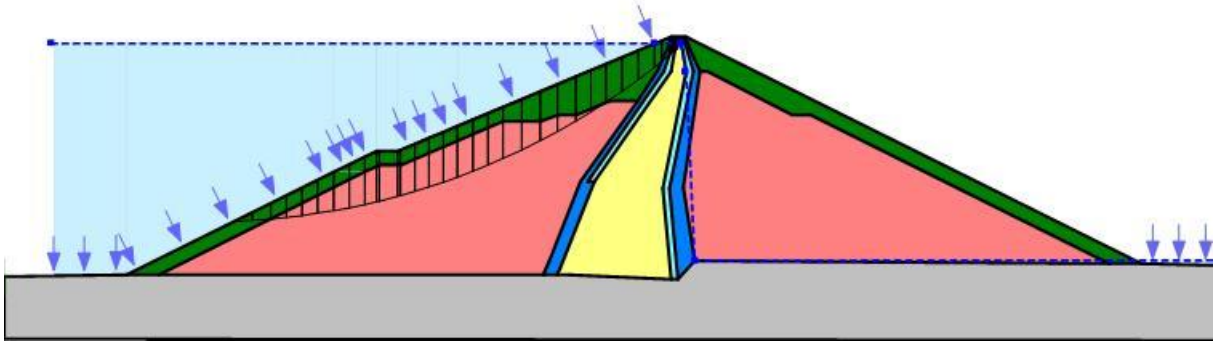

Figure 5.15 : Critical slip circle - Load case 2 - Cross section 1-3 upstream (FS=2.37)

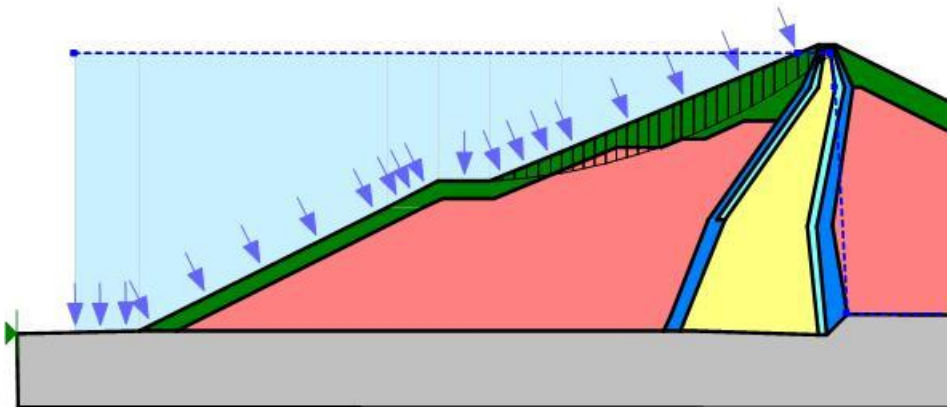

Figure 5.16 : Critical slip circle - Load case 2 - Cross section 1-4 upstream (FS=2.49)

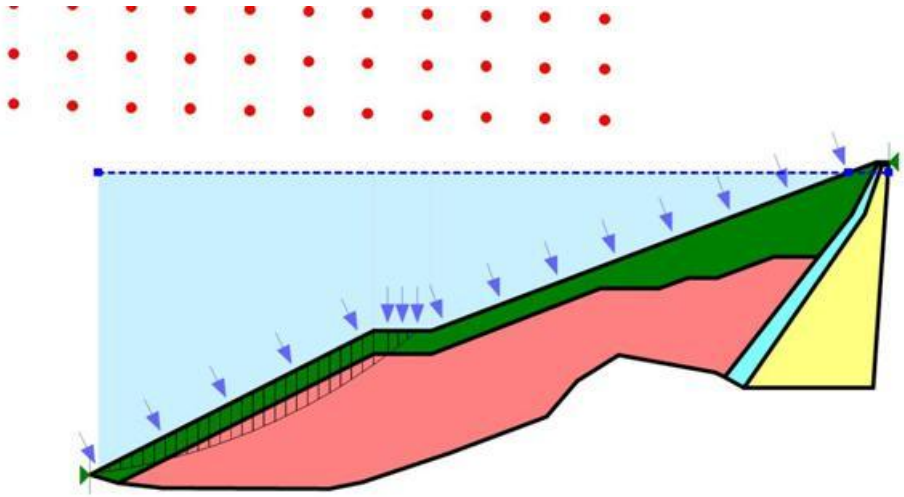

Figure 5.17 : Critical slip circle - Load case 2 - Cross section 1-5 upstream (FS=1294)

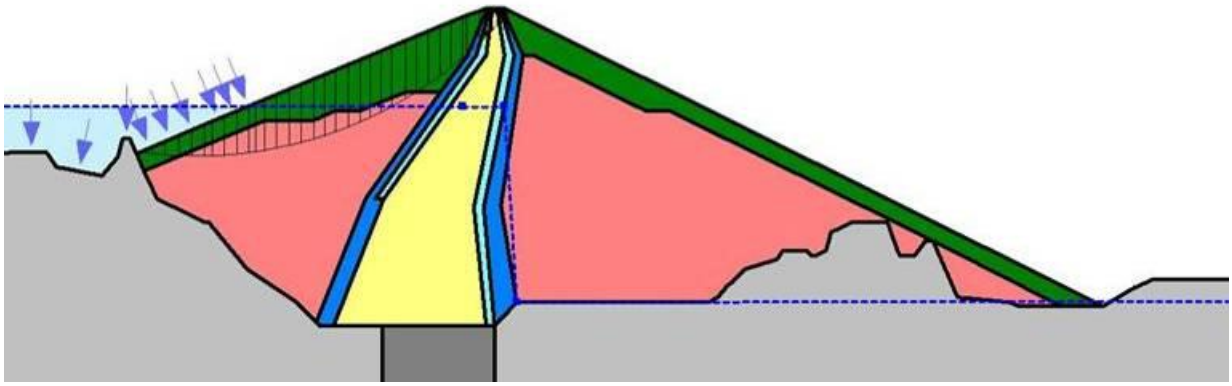

Figure 5.18 : Critical slip circle - Load case 3 - Cross section 1-1 upstream (FS=2.16)

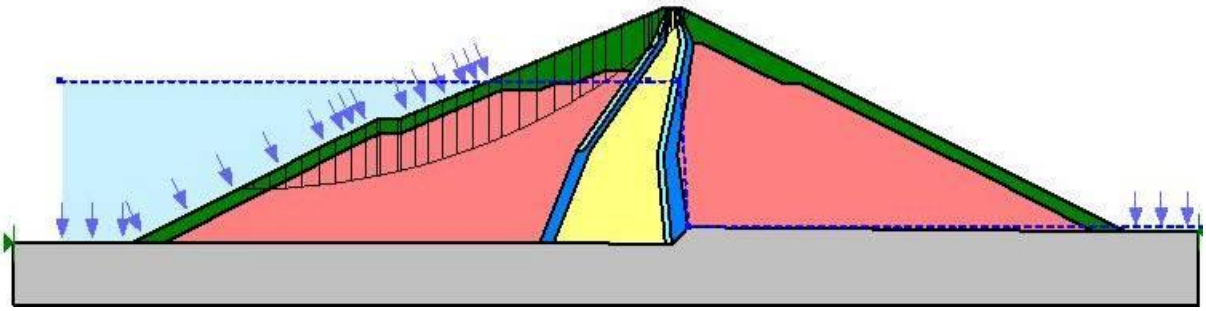

Figure 5.19 : Critical slip circle - Load case 3 - Cross section 1-3 upstream (FS= 2.12)

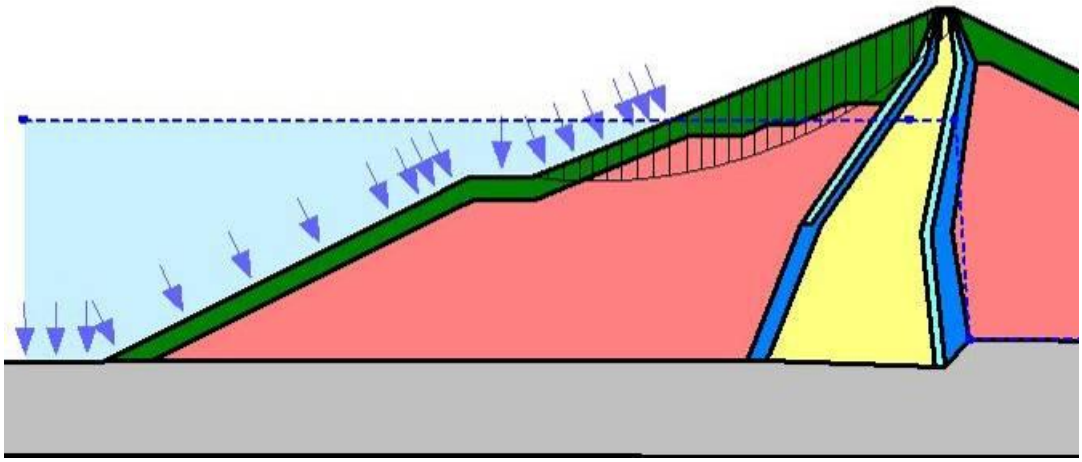

Figure 5.20 : Critical slip circle - Load case 3 - Cross section 1-4 upstream (FS=2.15)

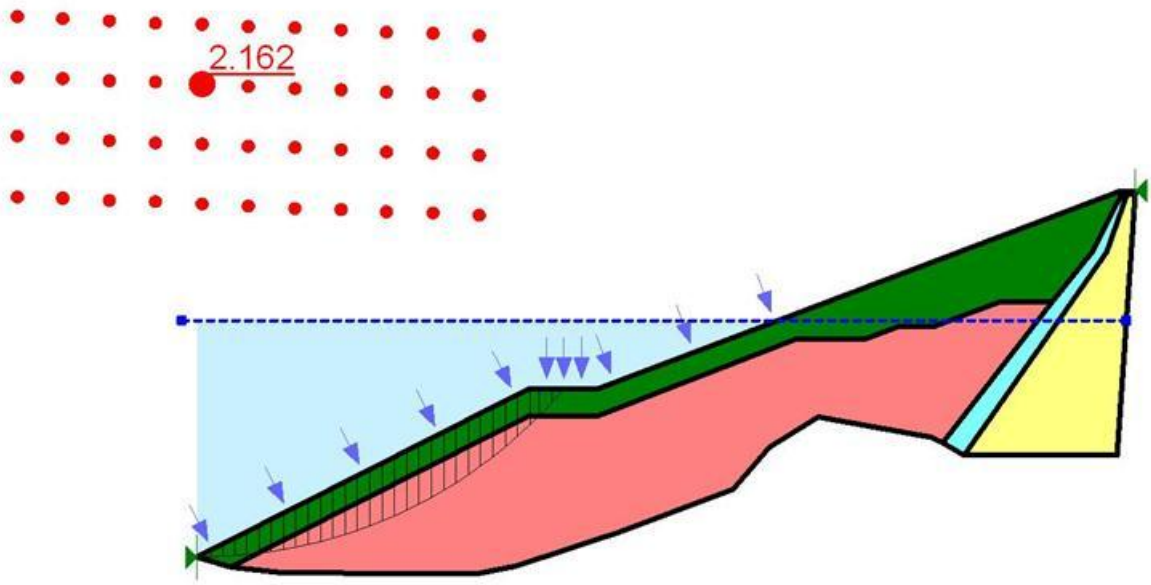

Figure 5.21 : Critical slip circle - Load case 3 - Cross section 1-5 upstream (FS=2.16)

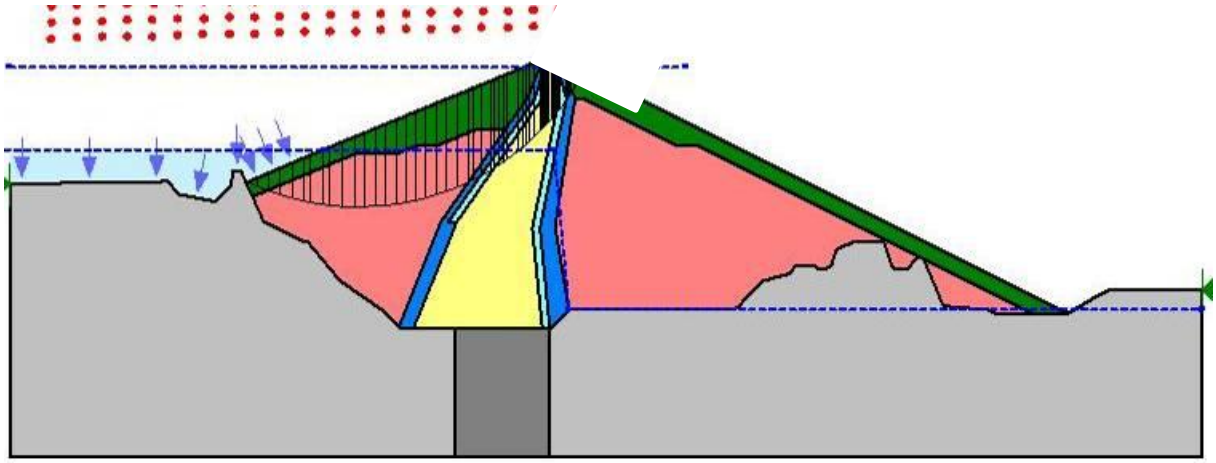

Figure 5.22 : Critical slip circle - Load case 4 - Cross section 1-1 upstream (FS=2.08)

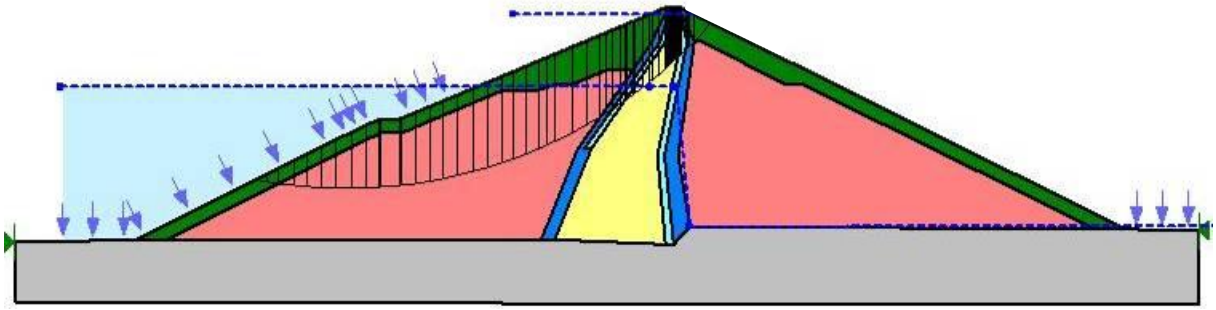

Figure 5.23 : Critical slip circle - Load case 4 - Cross section 1-3 upstream (FS=2.02)

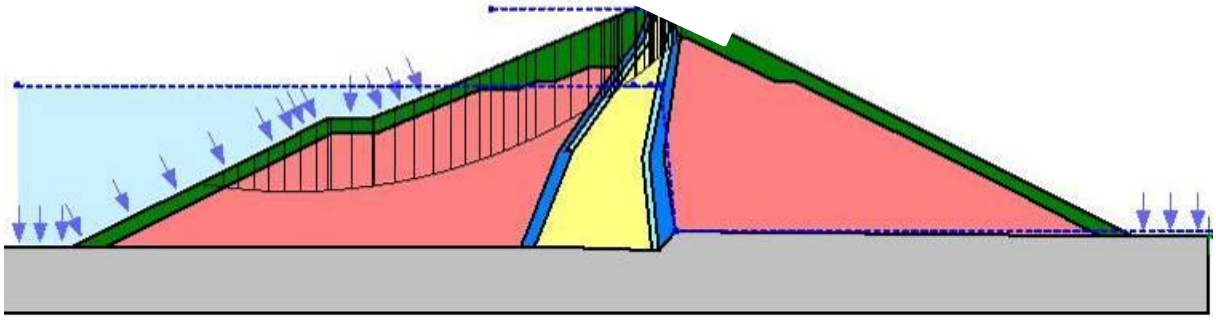

Figure 5.24 : Critical slip circle - Load case 4 - Cross section 1-4 upstream (FS=2.14)

5.5 Back analysis on the shear strength

The following figures display the effective normal stresses computed for two typical situations, representative of the whole spectrum of situations analyzed in the (static) stability study performed:

In Figure 5.25, the downstream stability for normal conditions with FSL (Figure 5.14 critical slip circle), where it can be seen that most of the shear resistance in the downstream shell is mobilized

in the range of normal stresses from 600 KPa to 1150 KPa - this range is displayed and numbered as (1) in Figure 5.4 and Figure 5.5 shown on the materials properties paragraph

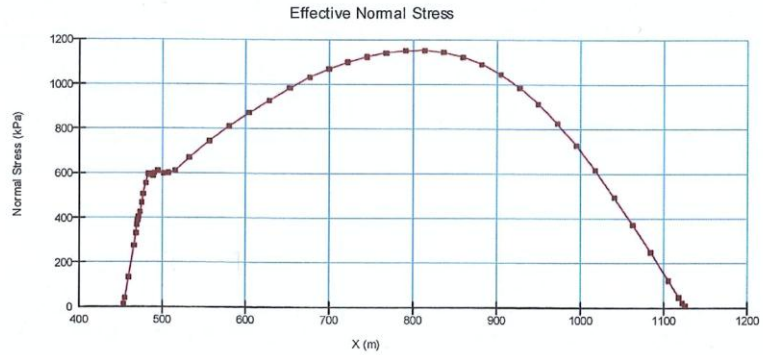

Values of normal stresses on 3 typical slices:

- **1142 kPa slice X= 730 (middle)**
- **1045 kPa slice X= 900 (lower third)**
- **617 kPa slice X= 1020 (toe)**

Figure 5.25 : Normal stresses for section 1-2 load case 2

And in Figure 5.26, the upstream stability for rapid drawdown from FSL to MOL (Figure 5.23 critical slip circle), where it can be seen that most of the shear resistance is mobilized in the range of normal stresses from 1800 kPa, to 2650 kPa - this range is displayed and numbered as (2) in Figure 5.4 and Figure 5.5 shown on the materials properties paragraph.

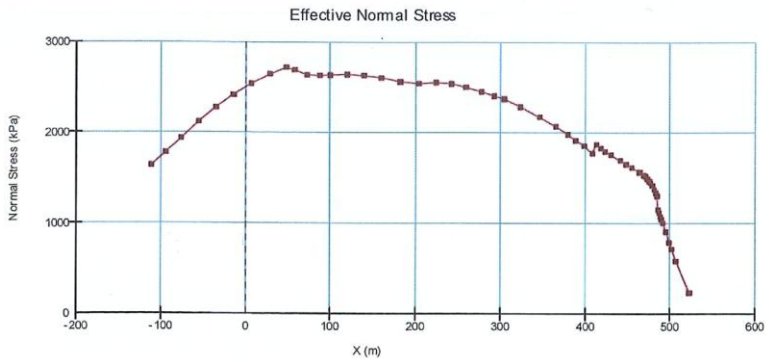

Values of normal stresses on 3 typical slices:

- **2503 kPa slice X= 240 (middle)**
- **2636 kPa slice X= 100 (lower third)**
- **2120 kPa slice x= -50 (toe)**

Figure 5.26 : Normal stresses for section 1-2 load case 2

For these ranges of normal stresses in Figure 5.4 and Figure 5.5, can be drawn the following comments and conclusions:

- For the downstream stability in normal conditions (range (1)), the assumed shear strength envelopes for Rogun Rockfill and Gravel shells materials, fall well in the core of the data in Figure 5.5, even if it looks somewhat on the low side in Figure 5.4, thus this situation appears globally satisfactory and do not deserve further comments;

- For the upstream stability in rapid drawdown conditions (range (2)), the assumed shear strength appear somewhat in the upper half of data in Figure 3, and above central trends on Figure 5.4, so this situation deserves some further comments;

- For this last situation, an evaluation can be drawn of the incidence on safety factor for the same slip line, should the shear strength assumptions to be corrected to fall right in the center of data range on Figure 3: the relevant secant apparent friction (gravel violet curve) should be reduced from about 40° to some 38° , so the resisting forces would be reduced in proportion of the Tangents of apparent secant frictions, and the Safety Factor would reduce from the computed value 2,02 to about

  SF= 2,02.(Tan 38° / Tan 40°)= 1,88

  which is still well above recommended limit values for that kind of situation.

In the comments presented above and in the material characteristics paragraph, the following conclusions have been drawn:

i) the assumptions made are reasonably relevant, compared with usual rockfills and gravels data, in the normal stress ranges computed in most of the stability analysis performed, and as most of the "critical" slip lines found are moderately deep, this relevance is secured for most of the situations assessed in the stability study performed;

ii) in the highest normal stress situation met in these stability analysis (the deepest "critical" slip lines evaluated), the assumptions appear somewhat in the upper half of data, so a correction may be evaluated to draw back the strength assumptions in the core of data, nevertheless the impact on the Safety Factor is moderate and do not affect critically this safety factor for this situation.

So, in our opinion, the relevance of the assumptions made is sufficiently secured at this stage of the studies, regarding both the representativity against shear strength data, and representativity against stress states range considered in the stability computations performed.

It is clear that in the next phases of the Project development such as the Detailed Design, given the exceptional size of Rogun Rockfill Dam, more in-depth stability studies will have to be performed, with curved shear strength envelopes, and reliability and sensitivity analysis (*7*). However, this will require specific data and tests results measured through a clear methodology, to get representative specific parameters, their mean values, dispersion coefficients or standard deviations, etc., which are not in the present scope of the study.

Furthermore, Rogun dam site configuration being strongly three-dimensional, not only because of its narrowness (*ratio width / height, or L/H, less than 2*) but also because of its tortuosity (*the site is quite curved in a plan view*), thus some consideration will have also to be paid on this subject and its benefits on global stability in the next phases of the Project.

7 *E. Frossard* « On the structural safety of large rockfill dams » *Proceedings XXIII° Intl. Congress On Large Dams , Q91-R39, (20p), Brasilia, May 2009*
Wu Z.Y., Li Y.L., Chen J.K., Zhang H., Pei L. " A reliability-based approach to evaluating the stability of high rockfill dams using a non-linear shear strength criterion" *Computers and Geotechnics 51, 42-49, May 2013*

6 SEISMIC ANALYSIS PERFORMED BY THE CONSULTANT

The seismic analysis contains first the pseudo-static analysis performed as a sensitivity tool, and then it presents:

- the criteria and assumptions specific to the dynamic analysis;
- the dynamic behavior of the dam thanks to the finite element model calculation (both with the elastic and the linear equivalent method);
- The assessment of the permanent displacements of the dam thanks to Swaisgood, Makdisi and Seed and Newmark method;

6.1 Pseudo static analysis – Sensitivity

This paragraph does not aim at assessing the safety of the dam under large seismic event. It is only used as a tool to evaluate the sensitivity of the dam to an additional horizontal gravity load.

This analysis is performed with the same methodology, geometry, and material characteristics as in the previous paragraph.

An additional horizontal load is defined in terms of horizontal acceleration. It is considered, as commonly assumed, that an average horizontal acceleration of 2/3 of the PGA is representative.

A sensitivity analysis is performed on this parameter, and the results are presented in the following graph.

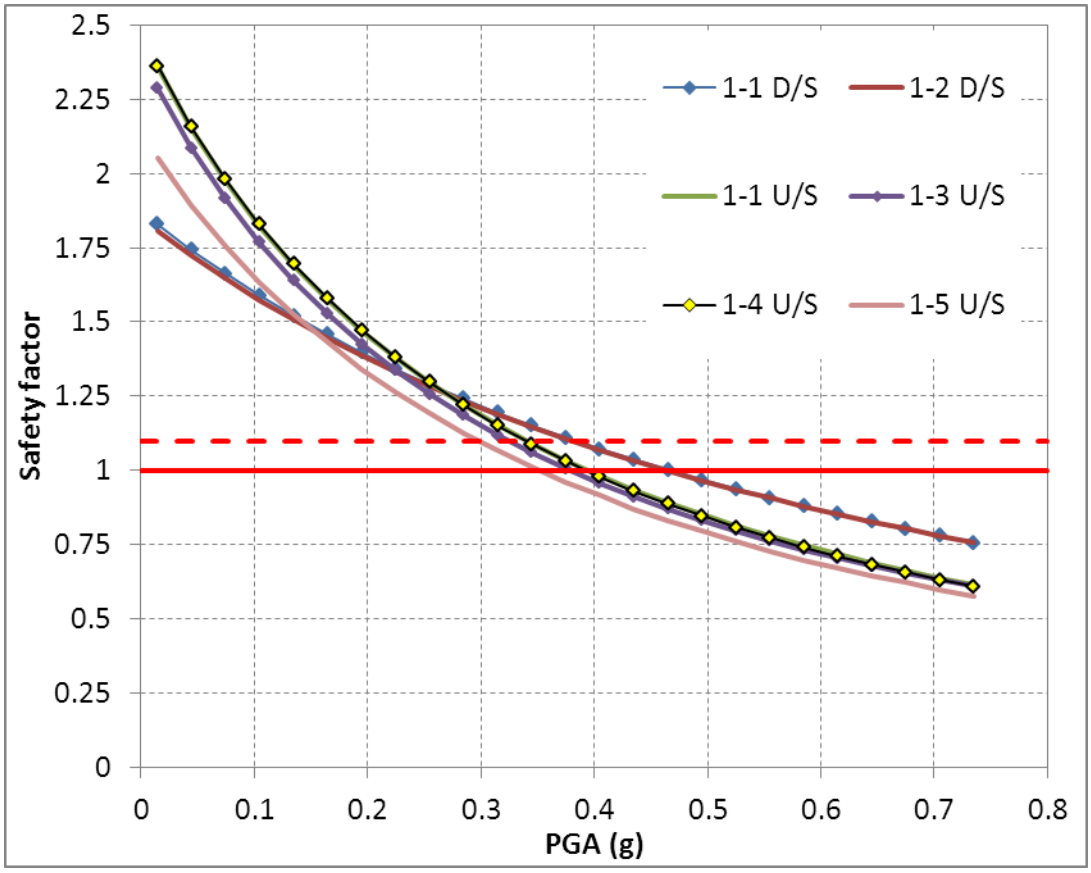

Figure 6.1 : Pseudostatic analysis - Sensitivity of the safety factor to the PGA

6.2 Design criteria

For the extreme seismic load case (MCE, Most Credible Earthquake), the dynamic behavior of the dam is studied and permanent displacements are then assessed. The vertical crest settlements are taken in to account on the freeboard design: the settlements likely to occur during an earthquake have to be lower than the available freeboard between the reservoir level and the dam crest.

The horizontal displacement shall be acceptable for the filters: their width shall be larger than the horizontal displacement during the MCE. The displacements calculated in this study will determine the filters width.

6.3 Geometry

The following cross sections are chosen to be studied in the seismic analysis:

- Cross section 2-1 is the section along the river bed;
- Corss section 2-2 is a “real” section along the right bank
- Cross section 2-3 is a “real” section along the left bank.

A plan view of these sections is presented in the figure below. It is worth to notice that section 2-1 represents the maximum dam section area. The two others are “real” sections on each bank.

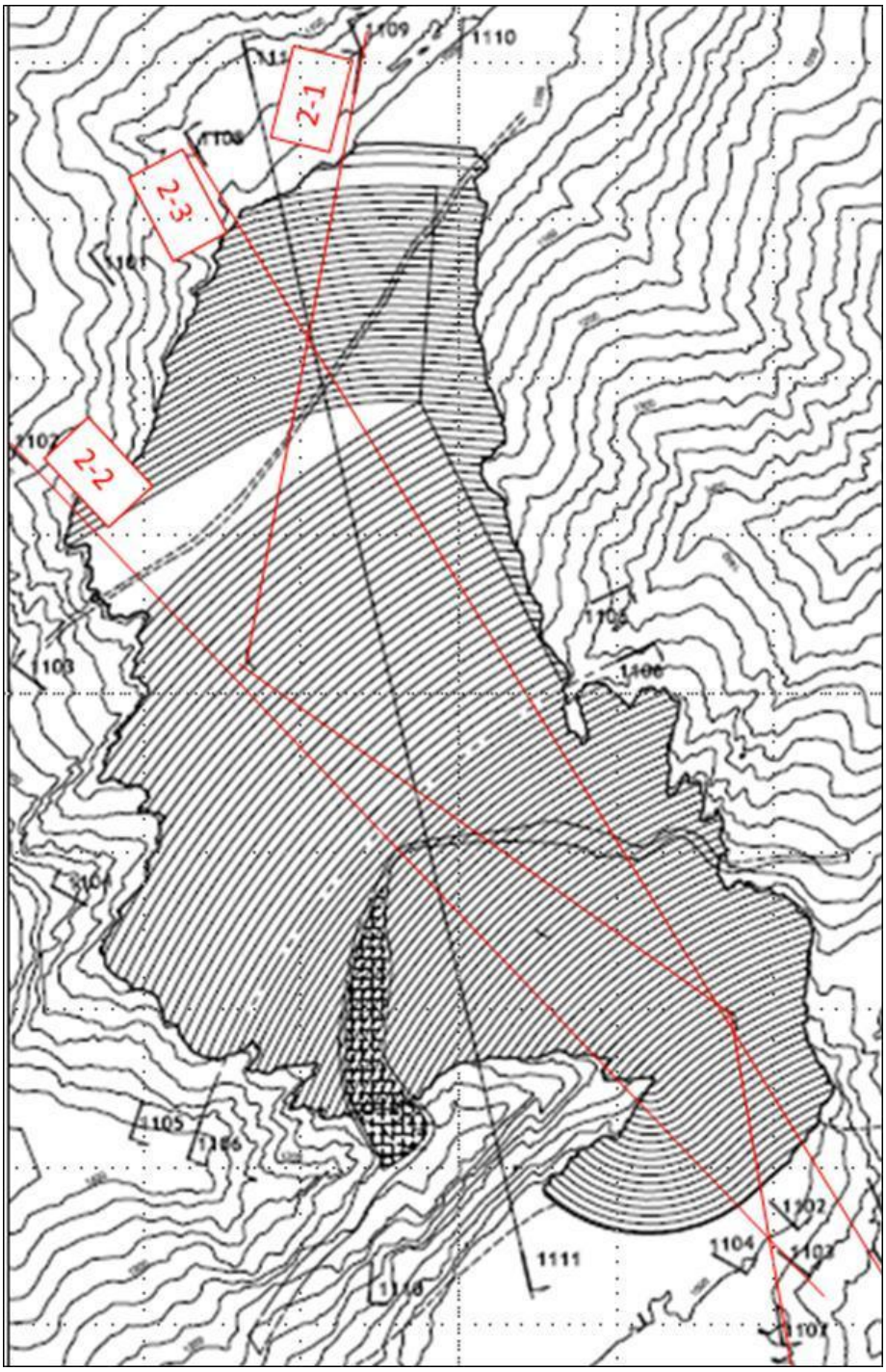

Figure 6.2 : Cross sections for dynamic analysis - Plan view

6.4 Design earthquake characteristics

As stated in the design criteria, the stability analysis during seismic loading are studied for the MCE (Maximum Credible Earthquake).

As defined in the Chapter 4 of Volume 2 – Seismicity, The Peak Ground Acceleration of the earthquake is presented in the following table.

Earthquake	PGA
MCE	0.71g

Table 7 : Design earthquake PGA

5 accelerograms have been used to produce the MCE. The figure below shows the spectra acceleration of the five accelerograms used to represent the input ground section. It can be seen that the range of fundamental period is 0.1-0.5 s.

The spectra used as excitation signal in the simulation is the Spectra 1 (black line).

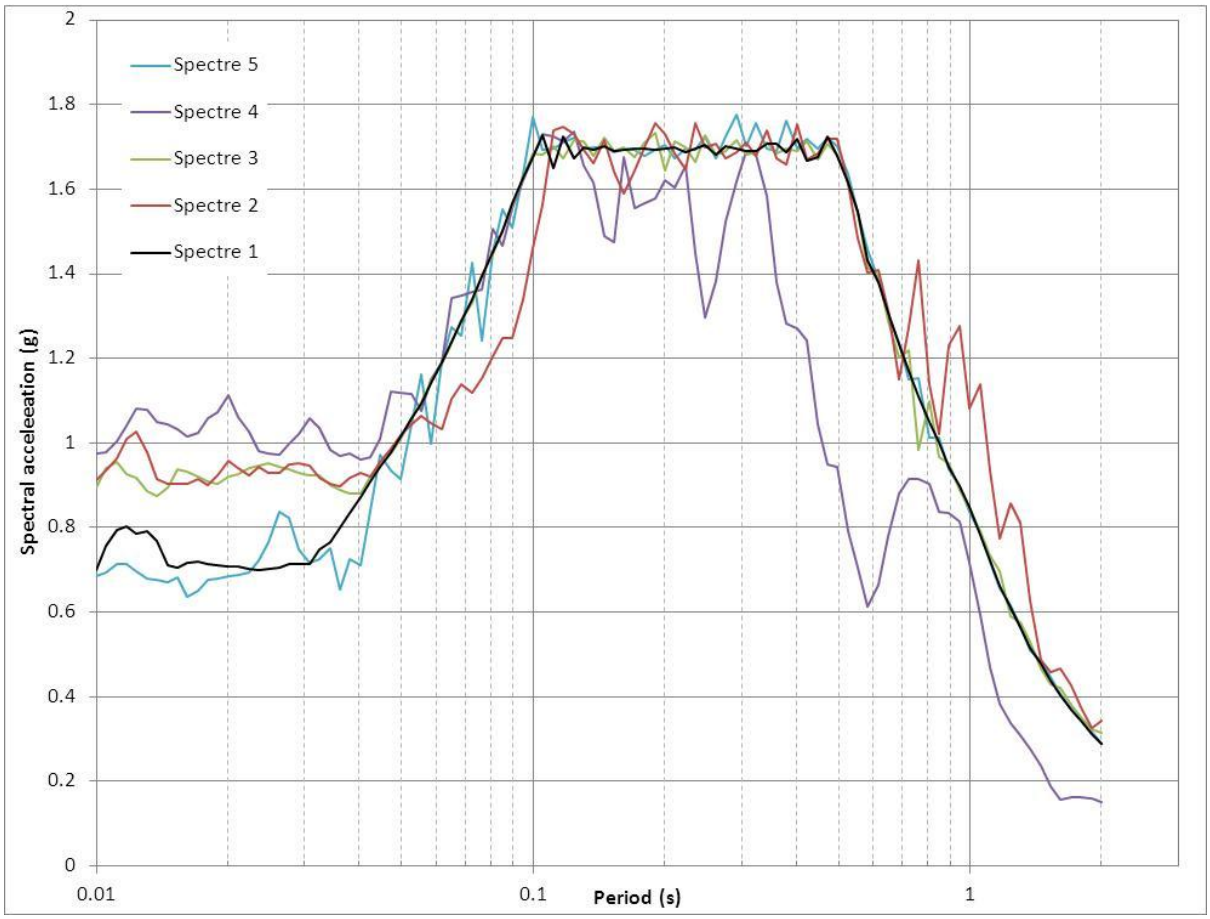

Figure 6.3 : MCE spectral acceleration distribution (damping ratio 5%)

6.5 Dynamic deformation parameters

Seismic response analyses using Quake software are performed assuming a visco-elastic stress-strain behavior of the materials. In addition, the equivalent linear approach iteratively calculates the elastic modulus and damping ratio of the material until they are compatible with the computed shear strains.

Elastic shear modulus, shear modulus reduction and damping curves are presented here after for the various zones of the dam body.

6.5.1 Small strain Shear modulus

The shear modulus is both stress and strain dependent. The shear modulus increases with the increase of effective confining stress and reduces with the increase of shear strain.

The small strain shear modulus is referred as G_{max} and can be estimated by the following formula [5]:

$$G_{max}(MPa) = 22.K\sqrt{P_a\sigma'_m}$$

$$\sigma'_m = \frac{\sigma'_v + k_0\sigma'_v + k_0\sigma'_v}{3}$$

Where P_a is the atmospheric pressure in kPa
and σ'_v is the overburden effective stress in kPa.

Material type	Rockfill	Gravel	Core	Fine filter	Coarse filter
K	180	180	70	70	70

Table 8 : Dam material characteristics - K value

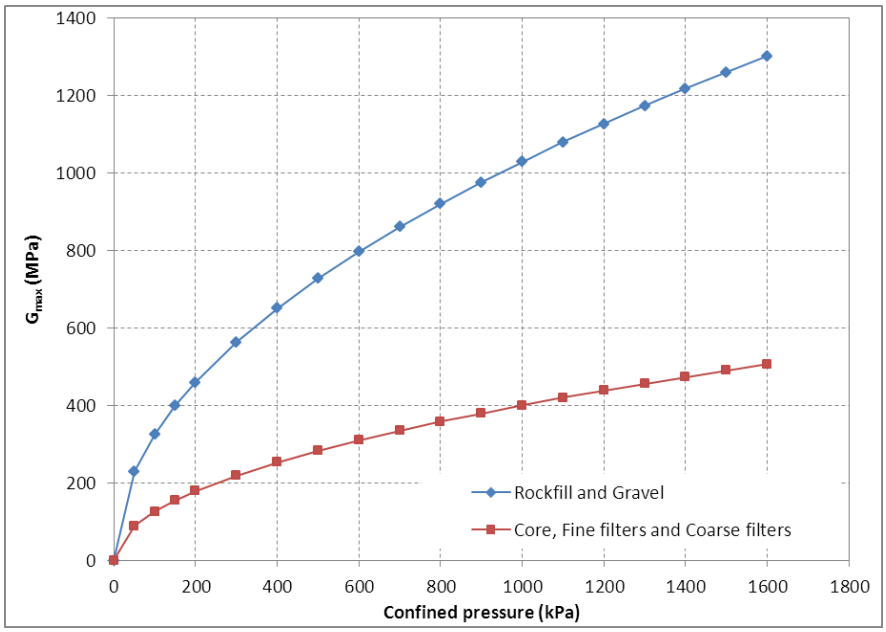

Figure 6.4: Dam material characteristic – Gmax

Given the unusual height of Rogun dam, high confined pressure can be reached. Therefore, at the bottom of the dam, the material shear modulus is higher than usual.

6.5.2 Shear modulus reduction fonction

A soil supporting dynamic stresses tends to « soften » in response to cyclic shear strain. This softening is here described as a ratio relative to $G_{max.}$. It is the G-reduction function.

Ishibashi and Zhang (1993) developed an expression for assessing the G/G_{max} ratio that is reminded below.

$$\frac{G}{G_{\max}} = K\ \gamma, PI\ \ \sigma'_m{}^{\,m(\gamma,PI)-m_o}$$

$$K\ \gamma, PI\ = 0.5\left\{1+\tanh\left[\ln\left(\frac{0.000102+n\ \ PI}{\gamma}\right)^{0.492}\right]\right\}$$

$$m\ \gamma, PI\ - m_o = 0.272\left\{1-\tanh\left[\ln\left(\frac{0.000556}{\gamma}\right)^{0.4}\right]\right\}\exp\ -0.0145PI^{1.3}$$

$n(\mathrm{PI}) = 0.00$ for PI = 0

$n(\mathrm{PI}) = 3.37 \times 10^{-6}\ \mathrm{PI}^{1.404}$ for 0 < PI < 15

$n(\mathrm{PI}) = 7.00 \times 10^{-7}\ \mathrm{PI}^{1.976}$ for 15 < PI < 70

$n(\mathrm{PI}) = 2.70 \times 10^{-5}\ \mathrm{PI}^{1.115}$ for PI > 70

Where PI, σ'_m, and γ are respectively the plasticity index, confining stress and cyclic shear strain.

Material type	Rockfill	Gravel	Core	Fine filter	Coarse filter
PI	0	0	0*	0	0

Table 9: Dam material characteristics - Plasticity Index

*: In reality, the Rogun core material is slightly plastic. But, it is considered that the sand-gravel part play a predominant part in the dynamic behavior of the material: at least 80% of the core material is made of larger than 80 µm elements.

6.5.3 Damping ratio

The damping ratio is a measure of energy dissipation; it increases with increasing magnitude of cyclic shear strain.

Ishibashi and Zhang (1993) developed an expression to calculate this parameter as following:

$$\xi = 0.333\frac{1+\exp\ -0.0145PI^{1.3}}{2}\left[0.586\left(\frac{G}{G_{\max}}\right)^2 - 1.547\frac{G}{G_{\max}} + 1\right]$$

The next figure shows the damping ratio curves for several confining pressure.

The formula shows that the damping ratio depends on the shear modulus which depends on the cyclic shear strain which itself depends on the dynamic response of the dam.

The three variable Shear modulus, damping ratio and cyclic shear strain are linked and an iterative method is necessary to solve the problem.

6.5.4 Comments on the dynamic material properties

The maximum shear modulus values used in our study are based on:

- the widely used reference formula proposed by Seed and Idriss in 1970, and further documented later, which is simply translated here in MPa units (instead of psf);

- the use of material coefficient ("K") values consistent either with systematic measurements on various materials as compiled by Seed, Idriss & al. in 1984, or with the coefficients computed by back-analysis of a very large dam response to an induced earthquake performed on Oroville Dam (234m in height, 60 millions cum. materials, end of construction 1967, California) landmark in the history of dams, specially interesting because of its zoning similar to the one of Rogun Dam, and its wide instrumentation.

The shear modulus reduction function and the damping ratio function developed by Ishibashi and Zhang (1993) have been calibrated on embankment dams and therefore appears representative for Rogun. However, the range of confined pressure used for the calibration is not in the range of the confined pressure found in the bottom of Rogun dam. None of the available bibliography deals with the same range of confined pressure as Rogun, which was expected given its unprecedented height.

The application of Ishibashi formula gives low damping ratio and high shear modulus for the mobilized cycling strain (G/Gmax is 0.9 and damping ratio 5% for cyclic strain of 0.3%). This is conservative in a sense that low damping ratio will increase dam amplification, and high shear modulus will lower the fundamental frequency and push it closer to the high amplification region of the response spectra. This assumption is therefore conservative in terms of estimated displacement. A sensitivity on the materials properties is performed later to address this issue and assess the variability of the results on these parameters (see § 6.7.5.2).

6.6 Dynamic dam behavior

6.6.1 Dynamic elastic behavior without the reservoir

As a first simplified approach, the fundamental frequencies of the dam body (section 2-1, 2-2 and 2-3) are estimated using the finite element code by MIDAS software and assuming an elastic linear behavior of the material and without the reservoir.

The first 30 natural frequencies have been calculated in order to warranty that at least 90% of the total mass is mobilized.

The following tables summarize the main natural frequencies and the total mass mobilized, the results for all 30 modes are presented in Appendix 1.

In order to take into account the variation of modulus as a function of the confining stress, the dam body is divided in various zones in accordance to their mean confining stress. The dynamic modulus has been assigned using the formula presented in §6.5.1.

Eigen value Analysis				Modal Mass participation (%)	
Mode No	Frequency	Frequency	Period	Horizontal - X	Vertical - Y
	(rad/sec)	(cycle/sec)	(sec)	MASS(%)	MASS(%)
1	5.16	0.82	1.22	58.93	0.03
2	7.64	1.22	0.82	0.01	26.31
5	10.37	1.65	0.61	15.94	0
6	11.73	1.87	0.54	0.02	16.56

Table 10: Principal natural frequencies of section 2-1

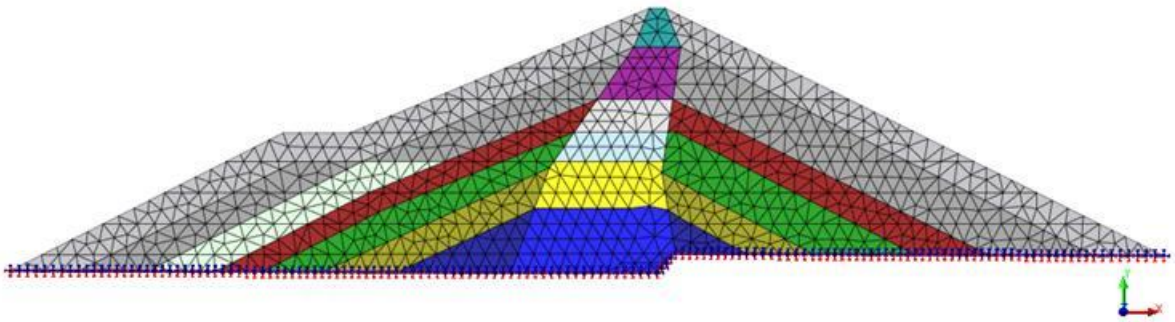

Figure 6.5 : Finite elements model for section 2-1

Eigen value Analysis				Modal Mass participation (%)	
Mode No	Frequency	Frequency	Period	Horizontal - X	Vertical - Y
	(rad/sec)	(cycle/sec)	(sec)	MASS(%)	MASS(%)
1	5.79	0.92	1.09	59.58	0.04
2	8.14	1.30	0.77	0.15	36.66
5	12.12	1.93	0.52	10.24	2.4
6	12.82	2.04	0.49	1.28	17.89

Table 11: Principal natural frequencies of section 2-2

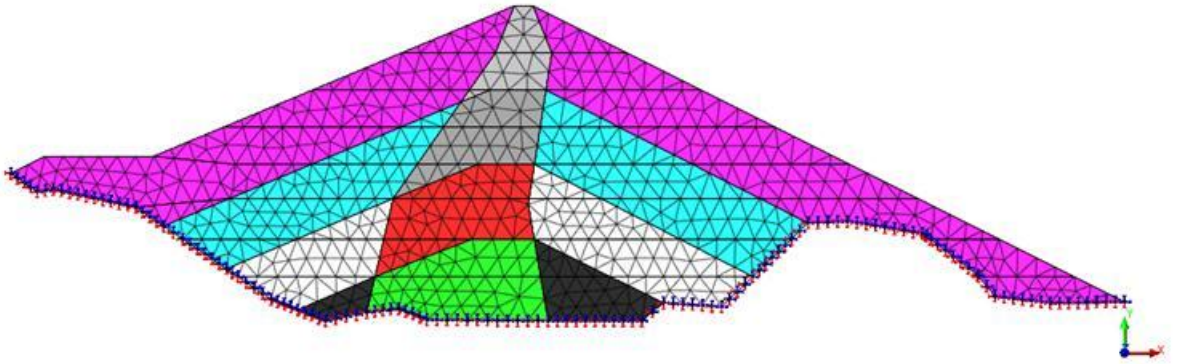

Figure 6.6 : Finite elements model for section 2-2

Eigen value Analysis				Modal Mass participation (%)	
Mode No	Frequency	Frequency	Period	TRAN-X	TRAN-Y
	(rad/sec)	(cycle/sec)	(sec)	MASS(%)	MASS(%)
1	8.01	1.27	0.78	36.19	0.15
2	11.20	1.78	0.56	0.03	15.22
3	12.50	1.99	0.50	24.15	0.33
8	17.49	2.78	0.36	0.31	17.06
10	18.20	2.90	0.35	3.52	13.65

Table 12: Principal natural frequencies of section 2-3

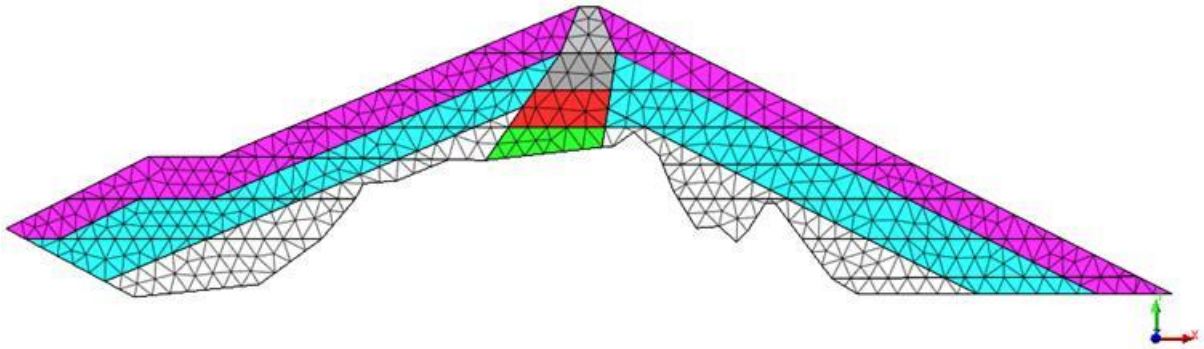

Figure 6.7 : Finite elements model for section 2-3

The first natural period of section 2-1 is 1.22 s, 1.09 s for section 2-2 and 0.78 s for section 2-3.

The first natural period of the dam is outside of the most amplificated range of period of the seism. Nevertheless, the third period and the following get closer.

6.6.2 Equivalent linear analysis

The linear equivalent analysis calculates the dynamic response of the dam to the earthquake. This is a temporal, equivalent linear, two-dimensional finite element computation performed with the Quake software.

The Quake model is constructed with the mesh geometry and the static stress field obtained by a stress analysis. The effective stresses are applied to estimate the maximum shear modulus (G_{max}) presented in section 6.5.1.

This analysis takes into account the elastic response, and also the soil strength softening with the strain, but it does not consider a plastic behavior of the material. The permanent deformations are evaluated afterwards according to the Newmark method.

The three section presented earlier are studied (2-1, 2-2, 2-3) with a reservoir at FSL. The Section 2-1 is also studied with an empty reservoir.

6.6.2.1 Fundamental period

The fundamental period of the dam body at section 2-1, 2-2 and 2-3 are estimated using the equivalent-linear Quake code by computing the horizontal harmonic response of the dam of a point located on the dam crest.

The horizontal harmonic response of the dam is calculated as the ratio between the Fast Fourier Transformation (FFT) of the crest response to the MCE ground motion. The main peaks represent the fundamental frequency of the dam.

It has to be highlighted that with a nonlinear or equivalent linear behavior of the material, the fundamental frequencies depend on the magnitude of the ground motion. Indeed, the earthquake amplitude reduces the shear modulus of the material (see §6.5.2), as a consequence the

fundamental frequency found should be lower than the one found with the elastic-linear computation.

It should also be noted that the reservoir effect is taken into account in this computation.

The first fundamental frequencies are reported in the next table.

As expected the first fundamental frequencies are slightly lower (periods are slightly higher) than the one found with the elastic analysis.

Section 2-2 and Section 2-1 have very close fundamental period and amplification, indeed the dam height under the crest is the same on those two sections. The fundamental period of section 2-3 is lower which is expected as its height is also much lower than the two other sections.

The amplification of the section 2-3 is higher than the others. Indeed, its fundamental period is closer of the fundamental period range of the MCE than the two others.

	Section 2-1	Section 2-2	Section 2-3
First fundamental frequency (Hz)	0.70	0.77	1.14
First fundamental period (s)	1.44	1.30	0.87

Table 13: Equivalent linear results - Dam fundamental frequency

6.6.2.2 Seismic response analysis

Here, the results are presented in terms of peak horizontal acceleration, effective peak shear stress and relatives displacements.

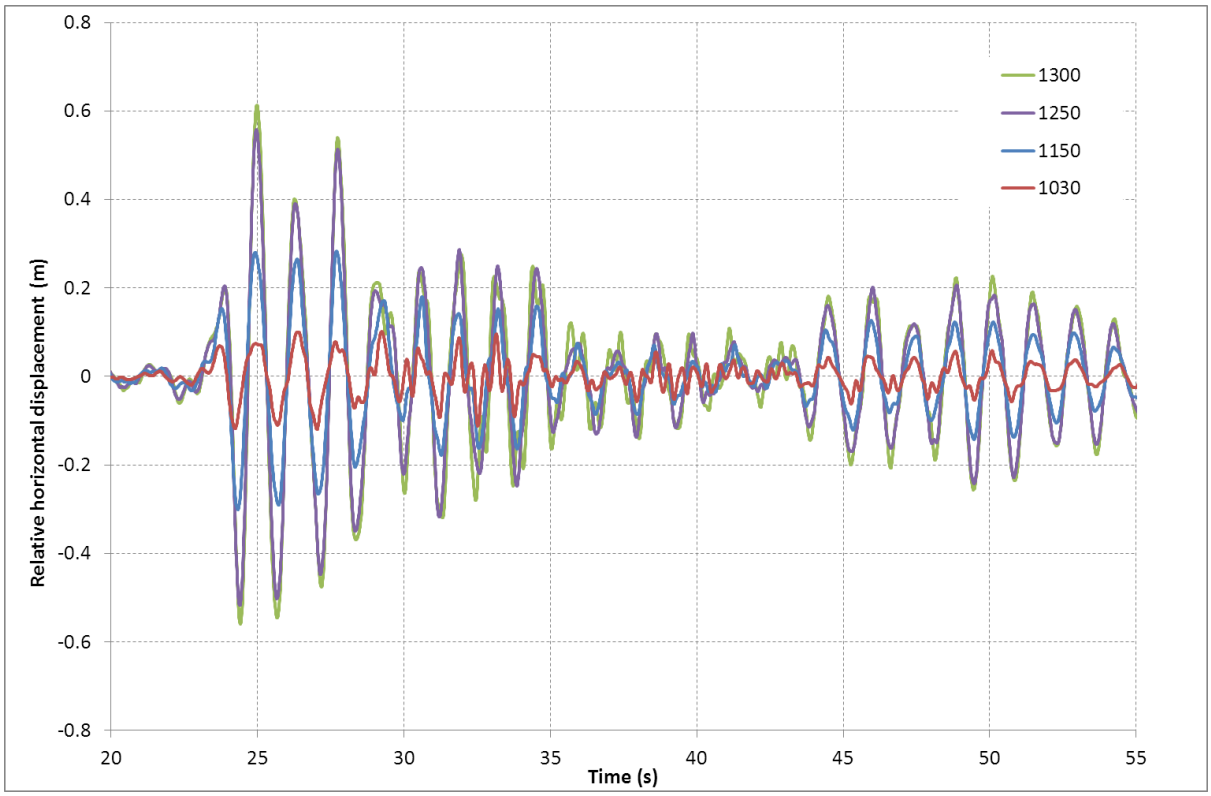

Figure 6.8 : Section 2-1, Relative displacement at several elevations

Figure 6.8 shows the time domain relative displacement of the dam thanks to several points located at various elevation of the central line of the dam body. It can be clearly seen that the peak takes place at the crest with a period in agreement with the first natural period found in §6.6.2.1.

Figure 6.9 shows the horizontal displacements, peak horizontal accelerations and strain profile through the centerline of the dam. Then, Figure 6.10 through Figure 6.15 present the contour plots of the peak horizontal acceleration and shear strain.

The following comments can be made about the results presented:

- Peak horizontal acceleration at the crest vary from 2.5g for section 2-3 to 3.76g for section 2-2.
- The larg risberm above the Stage1 dam is also an area of maximum peak acceleration. There , the peak acceleration vary from 3.3 to 4.3 g depending on the section.
- The peak horizontal acceleration contour lines tend to follow the upstream and downstream slope of the dam, and it decreases quickly within the dam.
- Finaly, the downstream toe of section 2-2 presents important horizontal acceleration: up to 3.7g.
- In the three section, the maximum peak effective shear strain is located 50 m under the crest and vary from 0.006 in section 2-3 to 0.0086 in section 2-2.

The seismic response analysis shows that the largest strains and largest crest acceleration are produced at section 2-2.

The peak horizontal acceleration contour shows where are the highest values: at the dam crest and at the larg risberm above the Stage 1 dam. The slip circle studied in the Newmark analysis should cross those area of high acceleration to found the most critical permanent displacement.

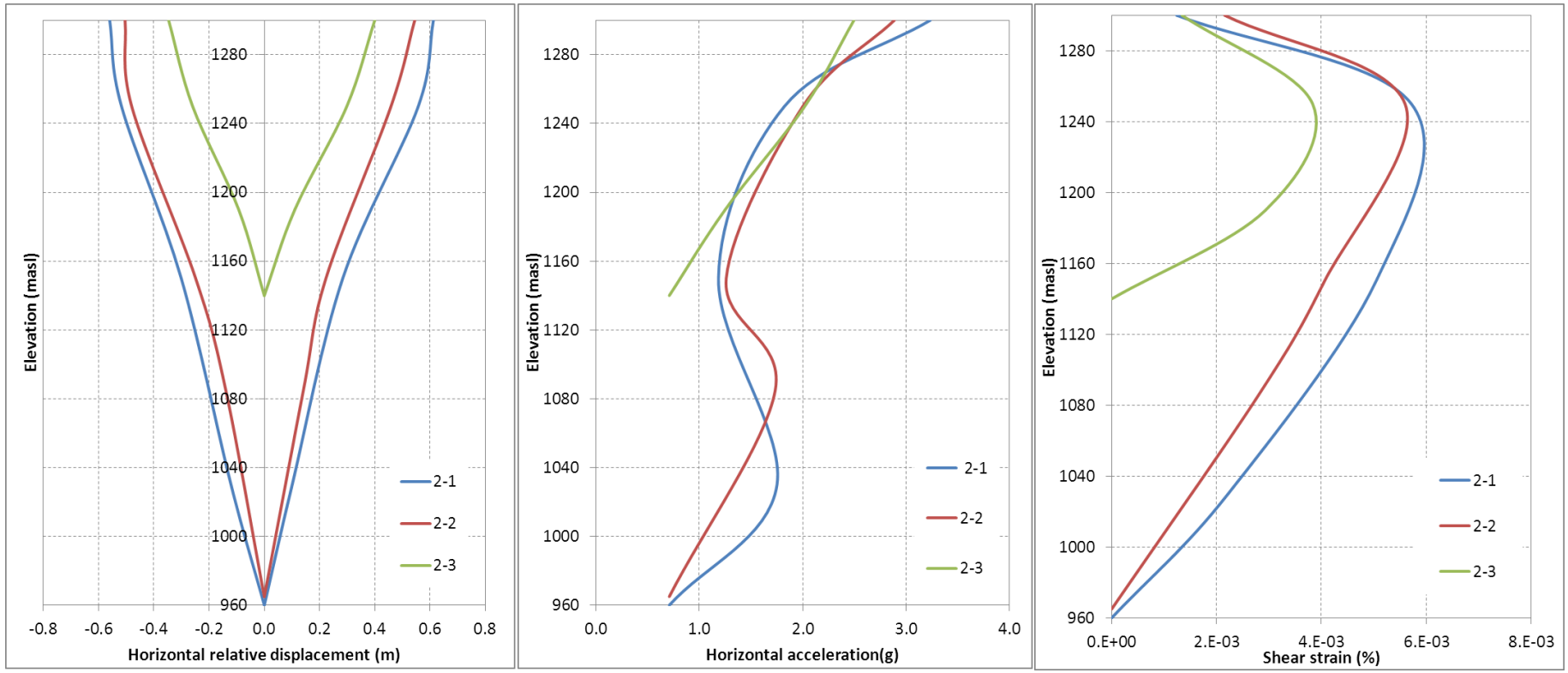

Figure 6.9 : Envelope of relative displacement, acceleration and shear strain – Vertical axis under the crest

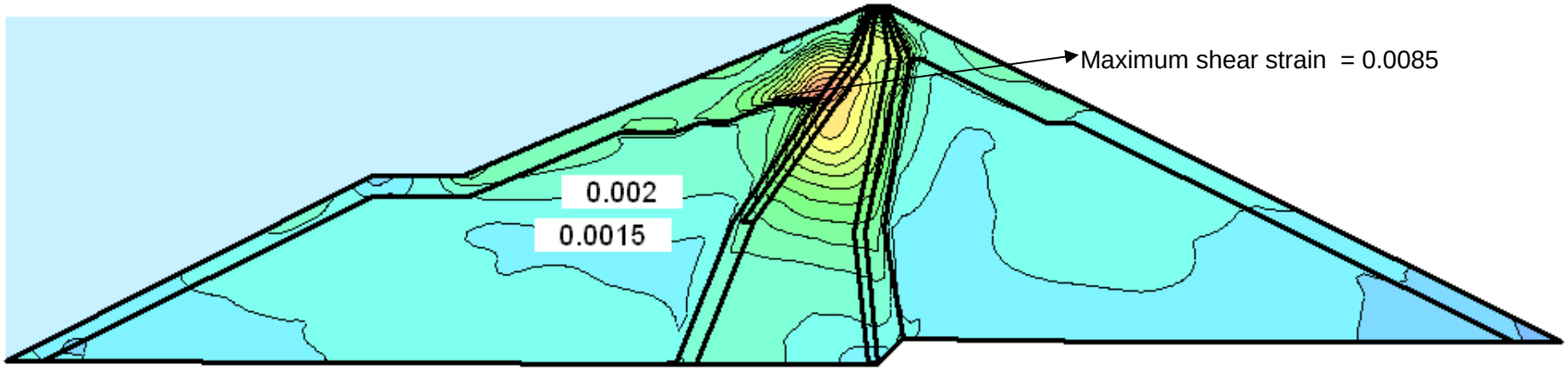

Figure 6.10 : Maximum Shear strain - Section 2-1

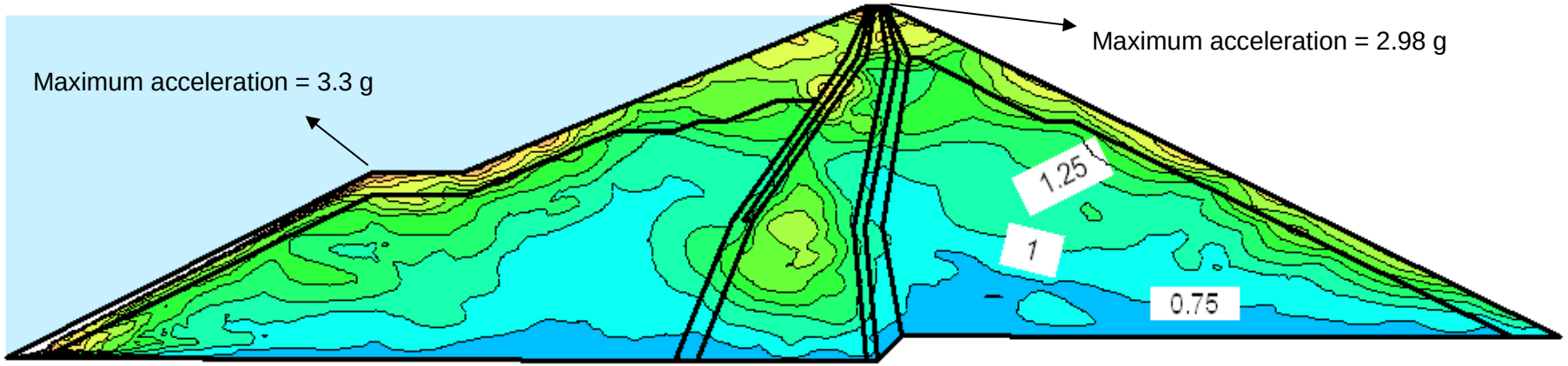

Figure 6.11 : Maximum horizontal acceleration - Section 2-1

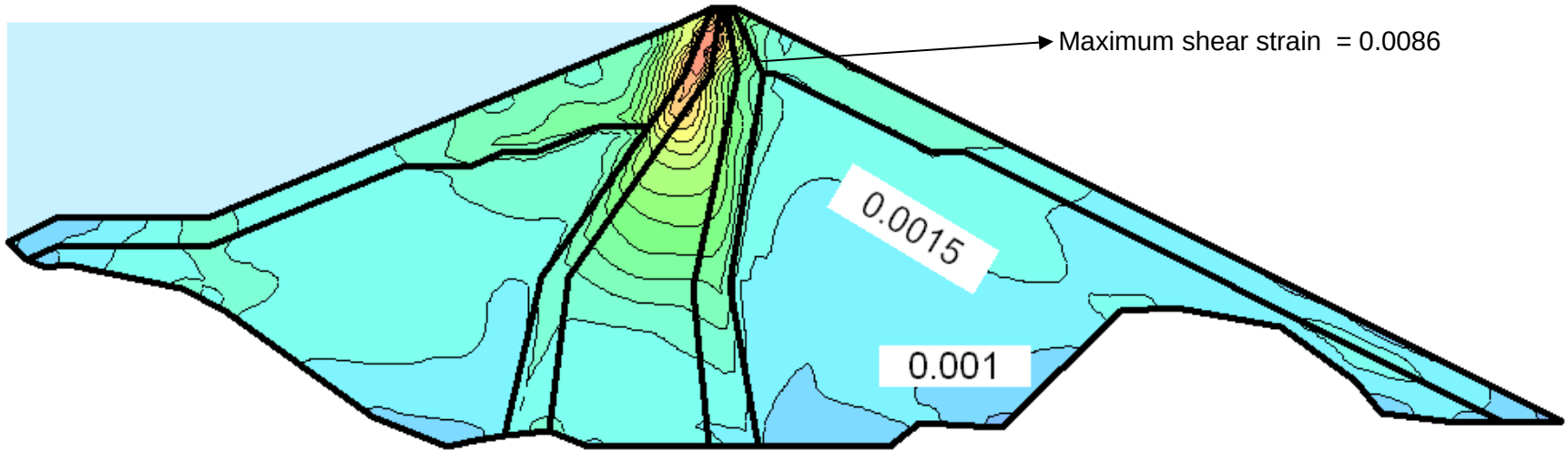

Figure 6.12 : Maximum Shear strain - Section 2-2

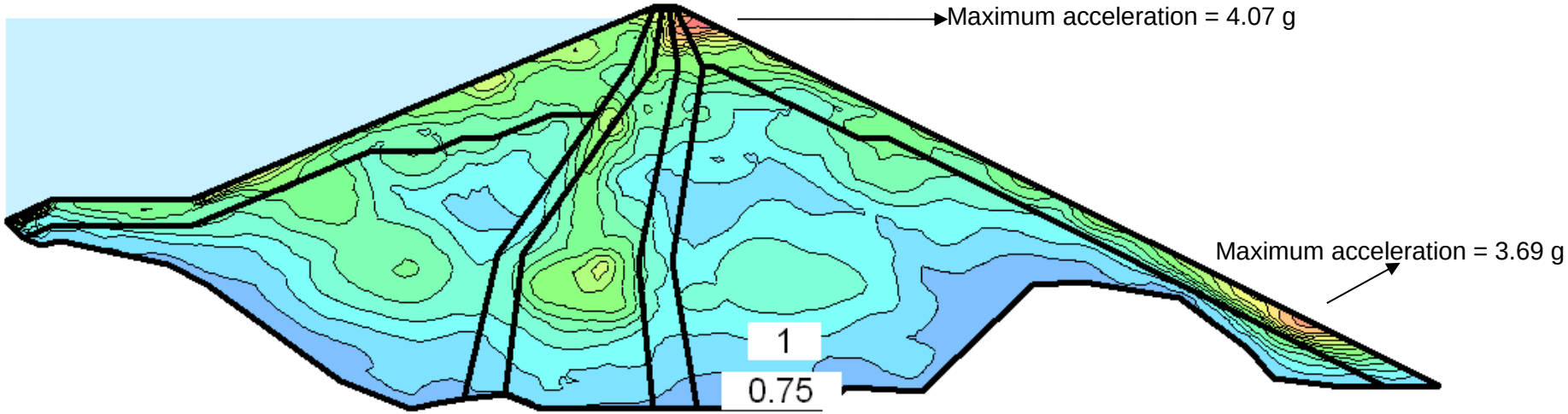

Figure 6.13 : Maximum horizontal acceleration - Section 2-2

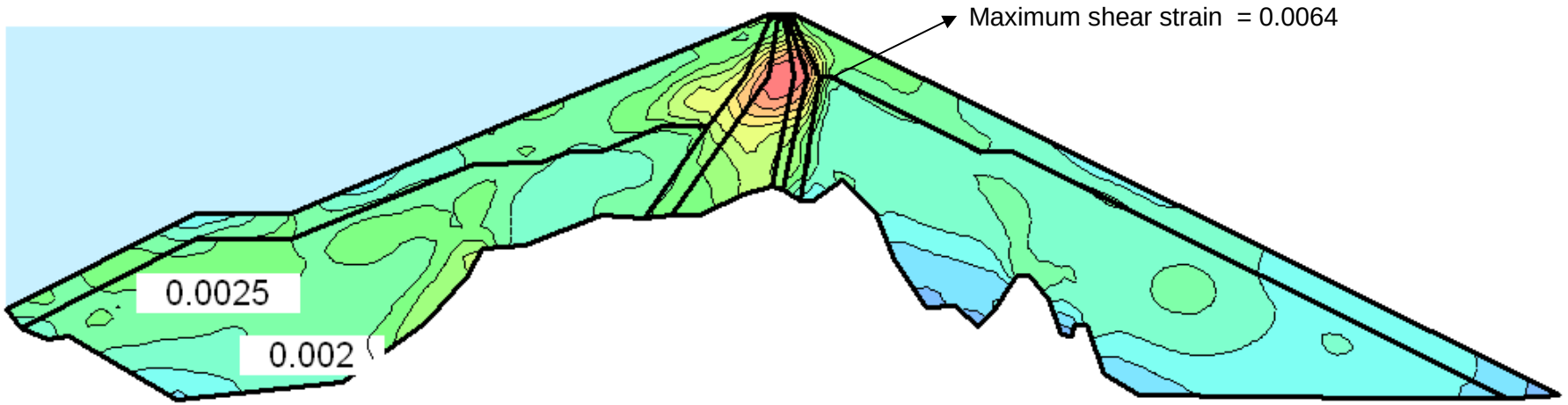

Figure 6.14 : Maximum Shear strain - Section 2-3

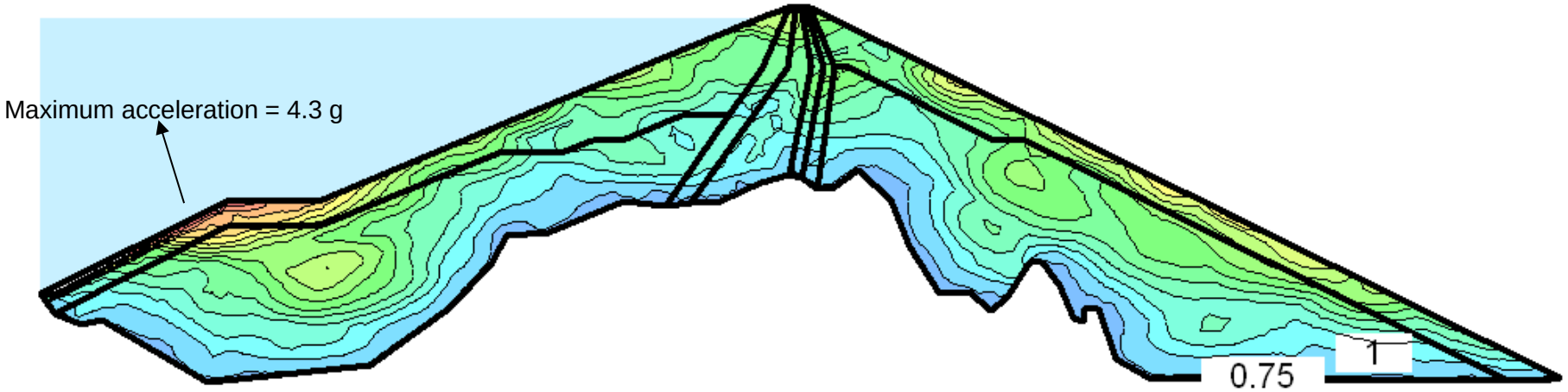

Figure 6.15 : Maximum Horizontal acceleration - Section 2-3

6.7 Assessment of permanent displacements

6.7.1 Swaisgood method

Based on the recorded seismic behavior of 69 embankment dams, J.R. Swaisgood developed an empirical equation to assess the maximum crest settlement. The relationship found links the maximum crest settlement (%) due to an earthquake to its magnitude (M) and Peak Ground Acceleration (PGA):

$$\frac{\Delta H}{H} = e^{(6.07PGA+0.57M-8)}$$

Assuming the maximum height of Rogun dam, and Maximum Credible Earthquake (MCE), the maximum settlement is:

Earthquake	PGA (g)	Magnitude	Maximum settlement (%)	Maximum settlement (m)
MCE	0.71	6.9	1.27	4.2

Table 14 : Swaisgood method – settlement due to MCE

6.7.2 Makdisi and Seed method

The method of Makdisi & Seed (1978) is a simplified procedure for assessing permanent displacement on the basis of the fundamental frequencies of the dam and yield acceleration.

The authors performed finite element modelisation and gathered others study results to build abacus that could be used by designers for permanent deformation assessment.

The maximum displacement is assessed thanks to the following abacus.

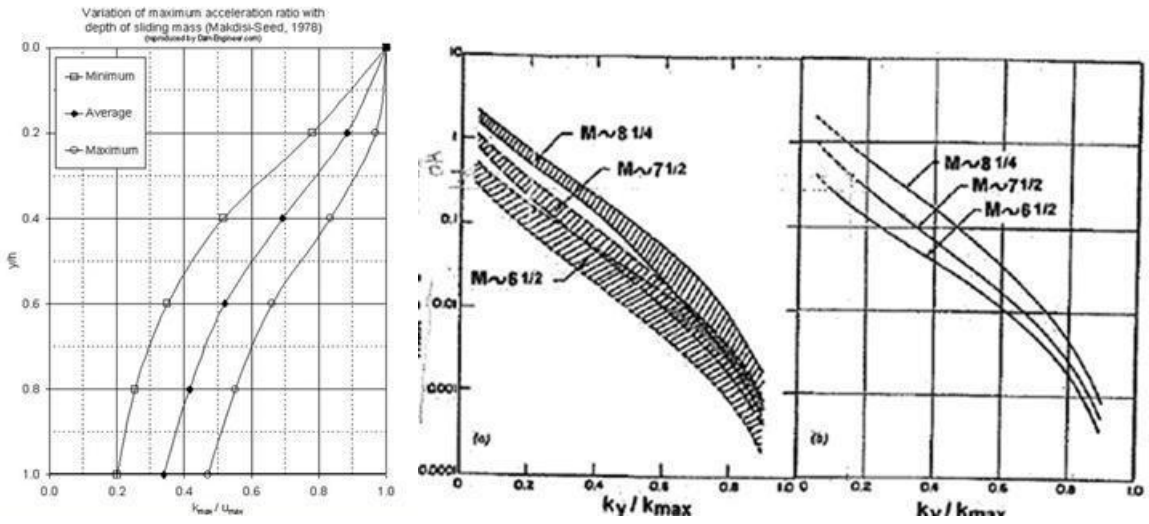

Figure 6.16 : Seed and Makdisi, 1977- Abacus

The method can be described by the following steps:

- By using a limit equilibrium analysis, the potential sliding mass and critical acceleration are determined. The critical acceleration that leads to a safety factor of 1 is the yield acceleration, and y is the depth of the base of the sliding mass;
- the maximal acceleration at the crest and the first fundamental period of the dam are determined;
- the figure on the left gives the maximum acceleration of the sliding mass at the depth y ($k_{max}g$);
- the figure on the right gives the permanent displacement of the potential sliding mass along the slip surface.

With the three cross section considered, the potential sliding mass and yield acceleration are calculated, and presented in the following table.

	UPSTREAM		DOWNSTREAM	
Cross-section	**Yield acceleration (k_c, g)**	**Circle depth (y, m)**	**Yield acceleration (k_c, g)**	**Circle depth (y, m)**
Cross-section 2-1 (along the Vakhsh River)	0.25	155	0.35	195
Cross-section 2-2	0.25	155	0.33	185
Cross-section 2-3	0.25	155	0.35	140

Table 15: Seed and Makdisi analysis data

Then, the maximum crest acceleration is calculated thanks to the following formula given by the authors:

$$\ddot{u}_{\max\_crest} = \sqrt{(1.65S_a(T1)^2 + (1.06S_a(T2)^2 (0.86S_a(T3)^2}$$

Where $S_a(T1)$, $S_a(T2)$, $S_a(T3)$ are the spectral acceleration of the three first fundamental dam frequencies. The first natural frequencies of the dam have been computed thanks to the linear equivalent modelisation. .

Then the permanent displacements along the slip circle likely to occur during the MCE are calculated thanks to the abacus. And finally, the displacement along the slip circle is decomposed in a vertical and a horizontal displacement.

Cross-section	**Displacement along the circle (m)**	**Crest settlement (m)**	**Horizontal displacement (m)**
Cross-section 2-1 (along the Vakhsh River)	9.7	5.7	8.0
Cross-section 2-2	10.3	6.1	8.6
Cross-section 2-3	2.5	1.5	2.2

Table 16: Seed and Makdisi analysis results - MCE

6.7.3 Newmark analysis

The Newmark method is implemented in the software Quake using a temporal dynamic in a linear equivalent modelisation. Once the temporal dynamic modelisation is run, the Newmark method is applied:

- A family of slip circle is assumed;
- For each time step calculated, an average acceleration of the potential sliding mass is calculated: the dynamic stress state is computed at the basis of each slice and a safety factor is calculated for each time step and each slip circle;
- the yield acceleration is found for each slip circle (the average acceleration for which the safety factor is unity).
- the area under the average acceleration versus time curve where the acceleration exceeds the yield acceleration is integrated twice to found the cumulative displacement of the sliding mass along the slip surface

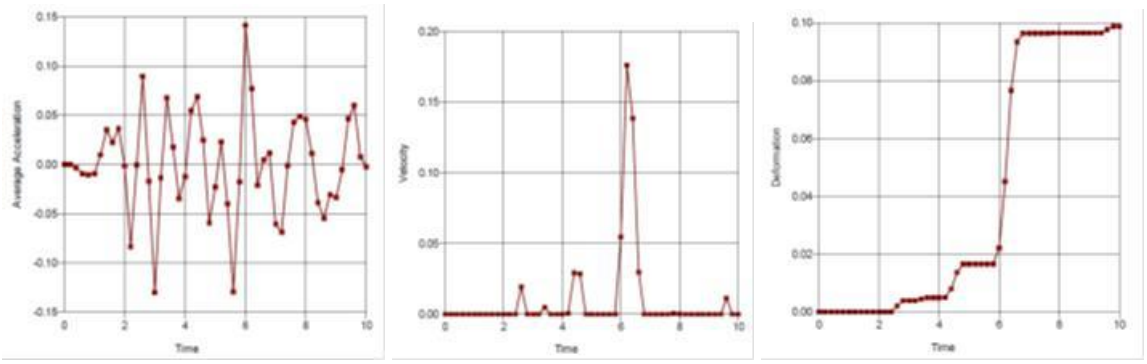

The Newmark method is applied to the three cross sections 2-1, 2-2 and 2-3. The next table presents the maximum displacements (along the slip surface, vertical and horizontal) found for each cross section studied during the MCE.

Section	Cumulative displacement along slip surface(m)	Horizontal displacement (m)	Vertical displacement (m)
2-1 (upstream)	9.8	9.0	5.3
2-2 (upstream)	8.5	7.8	4.2
2-3 (upstream)	10.2	9.1	6.0
2-1 (downstream)	3.8	3.8	0.3
2-2 (downstream)	3.9	3.9	0.8
2-3 (downstream)	3.7	3.3	2.2

Table 17: Maximum plastic deformation calculated with Newmark – MCE

It has to be noted that the horizontal displacement (shearing across filters) calculated for the three cross sections are in the same range, between 7 and 9 meters.

As expected, the upstream displacements are larger than the downstream displacement: the modelisation showed that accelerations were higher in the upstream shell, which could be explained by the fact that the effective weight is taken into account.

The slip circles that present the maximum displacement are presented in the next figures.

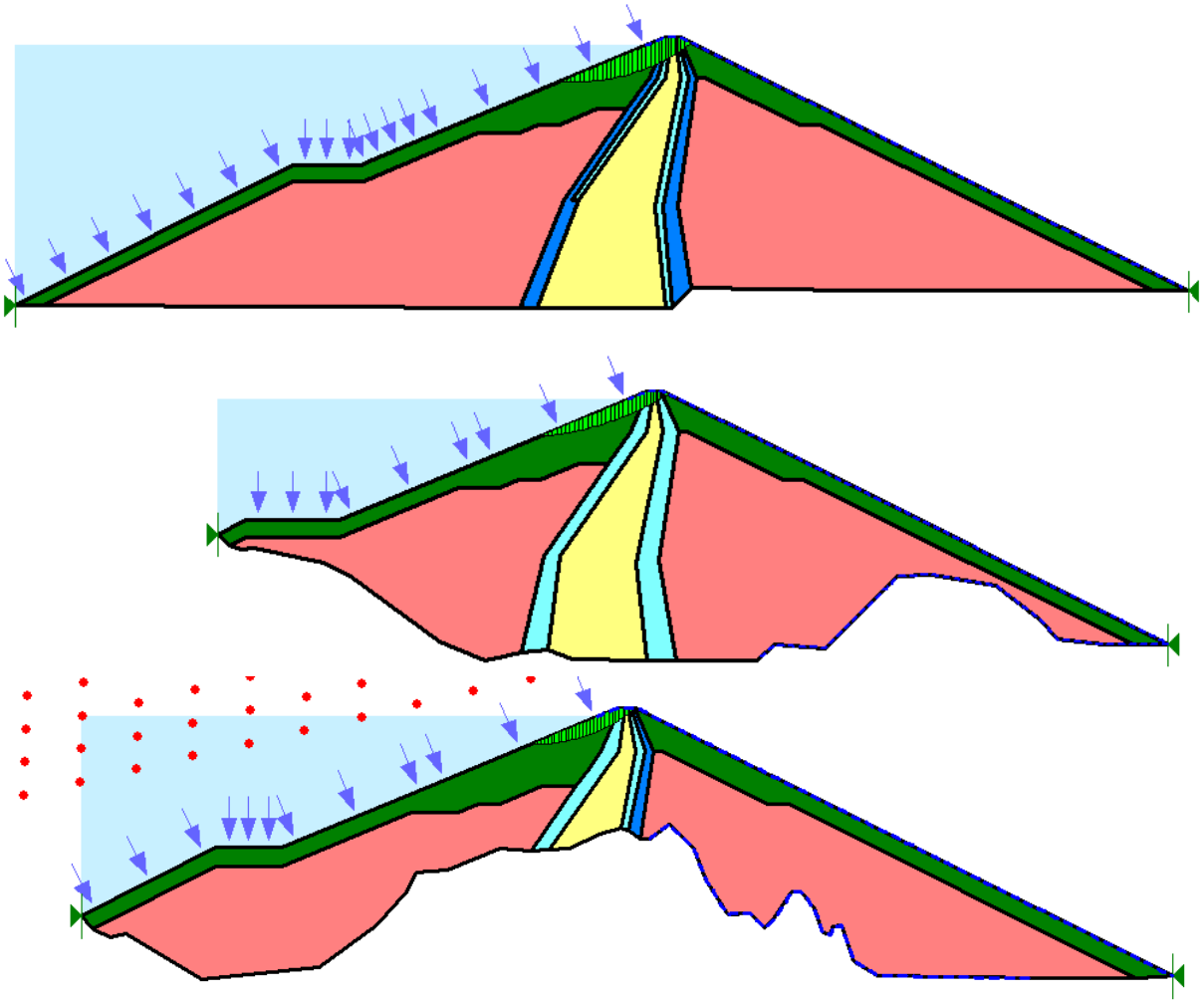

Figure 6.17 : Newmark analysis - Slip circles of maximum displacements – Section 2-1, 2-2, 2-3

Slip circles of maximum displacements are all located in the upper upstream part of the dam, and cross the core area. This is coherent with the results of the linear equivalent analysis where the map of maximum horizontal acceleration (Figure 6.11, Figure 6.13, Figure 6.15) indicates that the maximum values were on the crest, and along the upstream slope. On those figures, the Stage 1 crest was also an area of maximum acceleration, therefore, displacement in this area are also presented: the maximum displacement along the slip circle is 7.8 m, the matching slip circle is presented in the next figure.

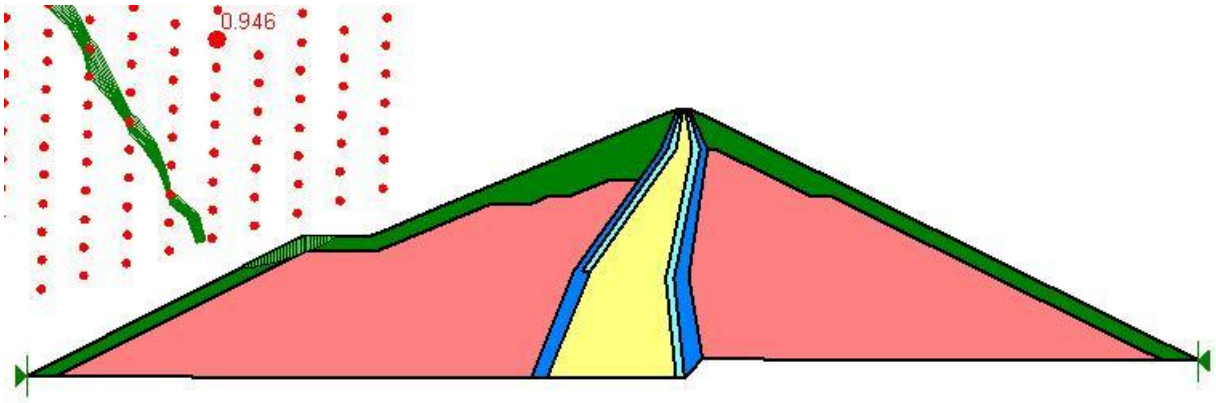

6.7.4 Synthesis on non-reversible displacements

The three methods presented before give several values of non-reversible deformation of the dam. The next tables compare those values of vertical displacement (settlement) and horizontal displacements.

Method	Section	Settlement calculated (m)
Swaisgood	-	4.2
Makdisi and Seed	2-1	5.7
	2-2	6.1
	2-3	1.5
Newmark	2-1	5.3
	2-2	4.2
	2-3	6.0

Table 18 : Results of Seismic analysis – Settlement

The various method applied give coherent results in term of crest settlement: between 1.5 and 6.1 m, with an average value of 4.7 m.

Method	Section	Horizontal permanent displacement calculated (m)
Swaisgood	-	-
Makdisi and Seed	2-1	8.0
	2-2	8.6
	2-3	2.2
Newmark	2-1	9.0
	2-2	7.8
	2-3	9.1

Table 19 : Results of Seismic analysis – Horizontal permanent displacement

The various method applied give coherent results in term of horizontal permanent displacement: between 2.2 and 9.1 m, with an average value of 7.5 m. One value is much lower than the others: section 2-3 with Makdisi and Seed method. The various cross sections give comparable results.

These values of permanent displacements are important but are consistent with the unprecedented size of the dam: it represents between 0.5% and 2.7% of the dam height. It is to be reminded that for the MCE, damages can be accepted as long as no uncontrolled release of water occurs.

Therefore:

- the range of settlement for the MCE is acceptable if at least a 6 m freeboard is provided.
- The range of horizontal displacements for the MCE is acceptable provided that filters are at least 10 m thick.

Repair works are to be planned after such high seismic event.

6.7.5 Representativity of the non-reversible displacements computed

6.7.5.1 Three-dimensional effect incidence

Rogun dam site configuration is strongly three-dimensional, not only because of its narrowness (ratio width / height, or L/H, less than 2) but also because of its tortuosity (the site is quite curved in a plan view). These features will participate in restraining the freedom of movements, and limit the internal transmission of dynamic forces, as in such configuration loads are partly transferred to the abutments instead of transmitting fully in dam body, producing what has been called by reference authors in this area a “stiffening effect of canyon geometry” (*8*) .

This three-dimensional effect in dynamic response of dams has been widely investigated in the past, and extensive comparisons between three-dimensional and plane strain two-dimensional dynamic analysis published in detail (ref 1 above,*9*). The main results are summarized in figures 6 and 7 here below:

8 *Mejia L.H., Seed H.B.* “ Comparison of 2-D and 3-D dynamic analysis of earth dams” *ASCE Journal of Geotechnical Engineering, Vol 109,N°11,1383- 1398, Nov1983*

9 *Kramer S.L. “* Geotechnical Earthquake Engineering*” Prentice –Hall, 1996, ISBN 0-13-374943-6*

- The stiffening effect of canyon geometry is far more marked for a triangular shaped canyon (as in Rogun site) than for a rectangular one, especially when the ratio L/H is lower than 2;
- For a triangularly shaped prismatic (not curved in plan view) canyon shape of the proportions of Rogun (L/H=1,92 approx.), the natural frequency of the first mode should be increased by a factor 2 approx., or the first natural period should be reduced by about 50%;
- This effect is far more marked on the first mode than on the others (Figure 6.19 right);
- These diagrams do not take account of further movement restraints brought by the site pronounced curvature in plan view, which will increase the stiffening effect of canyon geometry, leading to further reduction of the natural first period.

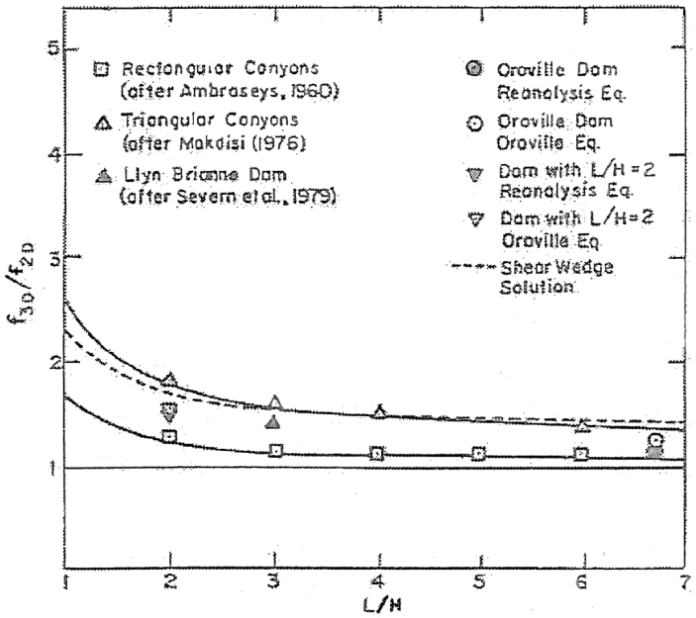

Figure 6.18 : Comparison between natural frequencies computed from 2-D and 3-D analysis of Dams in Triangular and rectangular canyons (extract from Mejia & Seed, ref 1)

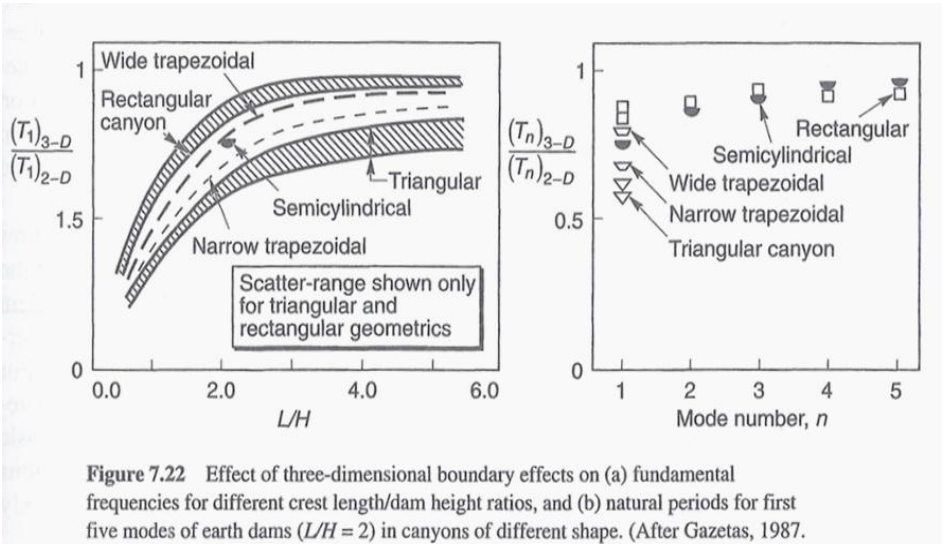

Figure 7.22 Effect of three-dimensional boundary effects on (a) fundamental frequencies for different crest length/dam height ratios, and (b) natural periods for first five modes of earth dams ($L/H = 2$) in canyons of different shape. (After Gazetas, 1987.

Figure 6.19 : Detailed comparison between natural periods computed from 2-D and 3-D analysis of dams in various canyons shapes (extract from Kramer, ref 2).

6.7.5.2 Sensitivity analysis on material properties

As explained in §6.5.4 on the materials dynamic properties, the base assumption for this study could appear conservative.

A sensitivity analysis has been performed using the section 2-1 and by changing the damping ratio function and the shear modulus reduction function. Two sets of characteristics have been used in this sensitivity analysis:

- The first set could be considered as an average of the various bibliography available (which means measured on confined pressure in the range of 50-300 kPa): G/Gmax is 0.1 and damping ratio 23% for cyclic strain of 0.3%;

- The second set is adapted from the first one by decreasing the damping ratio and increasing the shear modulus. Indeed, this is the expected effect of increasing confined pressure. It can be consider as an intermediate case between the base assumption and the first set: G/Gmax is 0.15 and damping ratio 12% for cyclic strain of 0.3%;

The first fundamental period found is 2.44 s for the second set and 2.85 s for the first set. As expected the fundamental period is higher when the material is less rigid (lower value of G/Gmax).

The maximum permanent displacement found (along the slip circle) is 1.5 m for the second set and 50 cm for the first set.

This shows that the study carried out at this stage is quite conservative and further analysis of material properties could lead to lower the values of displacement. On the other side, the 3D effect of the Rogun canyon can lead to a more rigid structure whose increased natural frequency gets closer to the high amplification area of the seismic response spectra, thus leading to higher values of displacements. This could be an optimization brought up by detailed design studies.

7 STAGE 1 STABILITY ANALYSIS

7.1 Geometry

As for the final dam, the Stage 1 dam geometry considered is the one proposed by HPI.

Indeed, the geometry and especially the slopes of the Stage 1 dam are imposed by topographical and site constrains. Those constrains are detailed in the dam design report: final dam core footprint, diversion tunnel intakes and Ionaksh fault.

This paragraph mainly aims at verified that the 1.7H/1V downstream slope and 2H/1V upstream slope verify the design criteria. It aims also to check the stability of the wedge shaped by the watertight membrane (which is replaced by a bituminous core in the Consultant design).

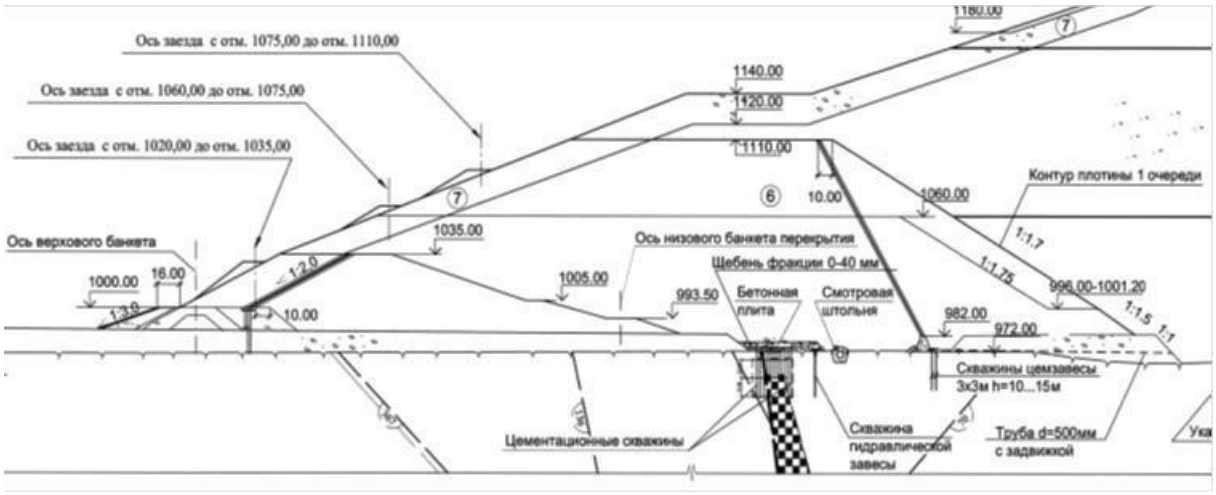

Figure 7.1 : Stage 1 dam geometry

7.2 Material properties

The Stage 1 dam is made of the same gravel material than the final dam, therefore its characteristics are identical than in §5.3.

The dam-foundation friction angle is considered as the lowest of the dam material internal friction angle and the foundation internal friction angle, ie 39° under the gravel shell.

7.3 Calculation method

As it is a step of construction, the stage 1 stability is only verified thanks to a 2D slope stability analysis.

	Loading condition	Minimum safety factor
1	End of construction	1.3
2	Normal condition - Water level at FSL	1.5

Table 20 : Design criteria for the Stage 1 dam

The wedge shaped by the watertight membrane is pushed by the water pressure acting on the membrane and the friction is mobilized on the horizontal surface. The stability of the wedge is assessed considering this wedge as rigid and by force equilibrium as illustrated in the next figure.

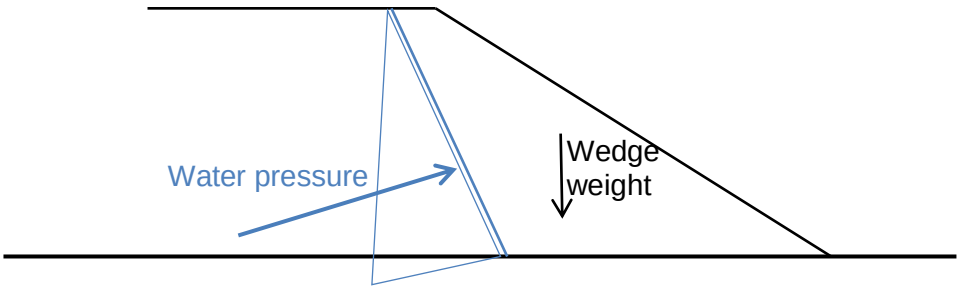

Concerning seismic event, MCE defined earlier is adapted to a stand-alone project. Here, the Stage 1 dam is a construction step that lasts less than 10 years. Two approaches are being used to assess the Stage 1 dam sensitivity to earthquake:

- The evaluation of the irreversible deformation thanks the Swaisgood formula;
- The research of the maximal horizontal acceleration that still respect a safety factor of 1.

7.4 Results

The critical safety factors for each load case are presented in the next table.

	Loading condition	Slope	TEAS results	HPI results
1	End of construction	Upstream	2.09	-
		Downstream	1.72	-
2	Normal condition - Water level at FSL	Upstream	2.20	-
		Downstream	1.70	1.56
		Wedge	2.53	-

Table 21 : Stage 1 dam stability analysis – Results

The next figures show the critical slip surface for each cross section and loading conditions.

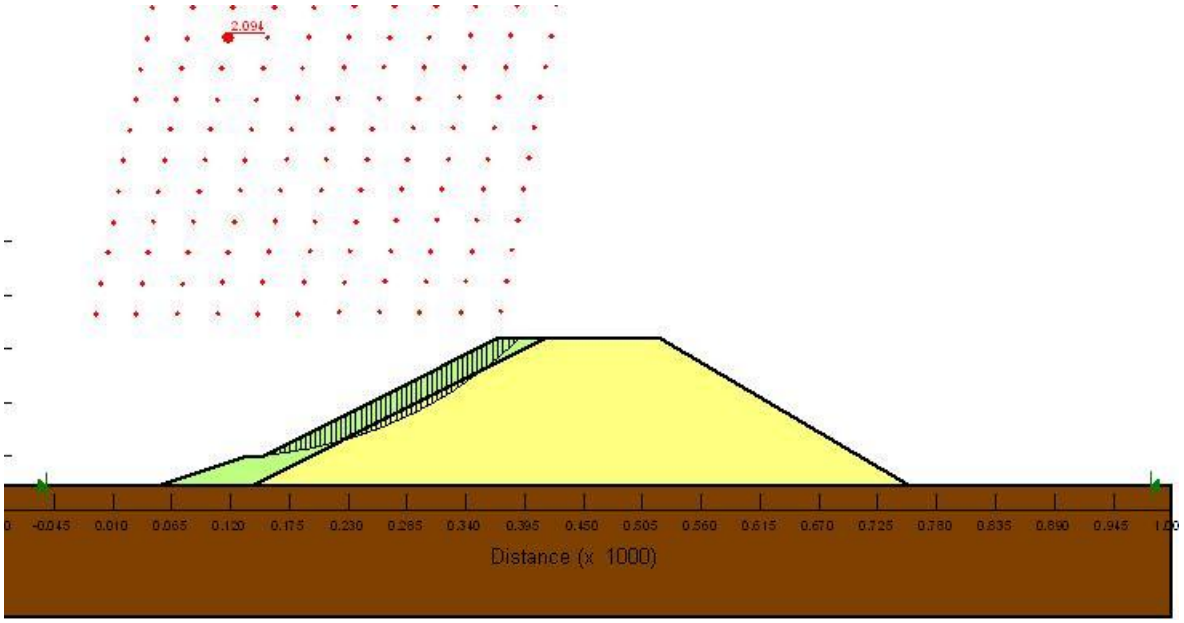

Figure 7.2 : Stage 1 critical slip circle - End of construction – Upstream (SF=2.09)

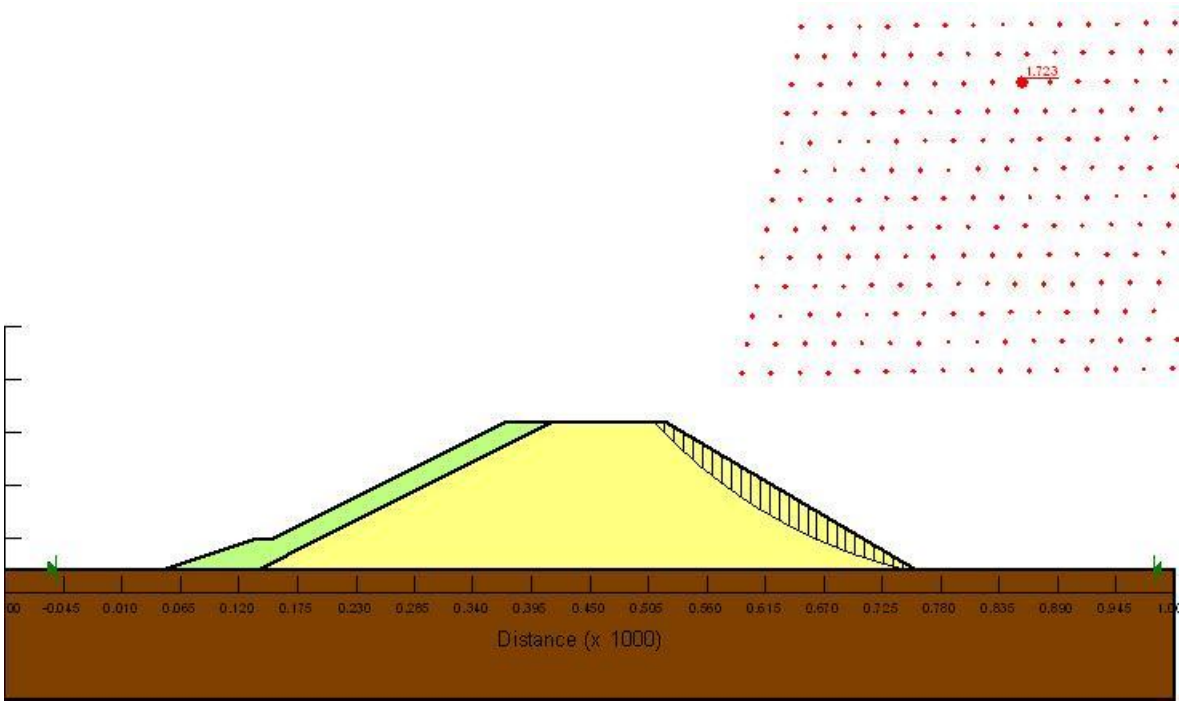

Figure 7.3 : Stage 1 critical slip circle - End of construction – Downstream (SF=1.72)

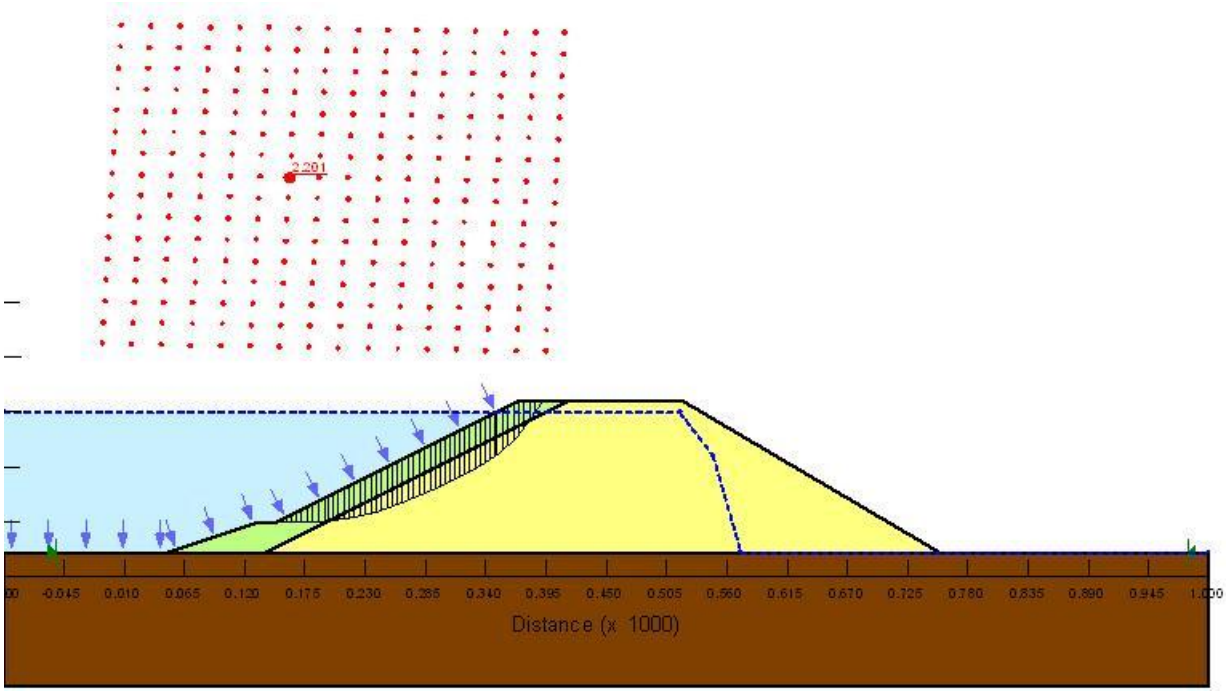

Figure 7.4 : Stage 1 critical slip circle – Normal water level – Upstream (SF=2.2)

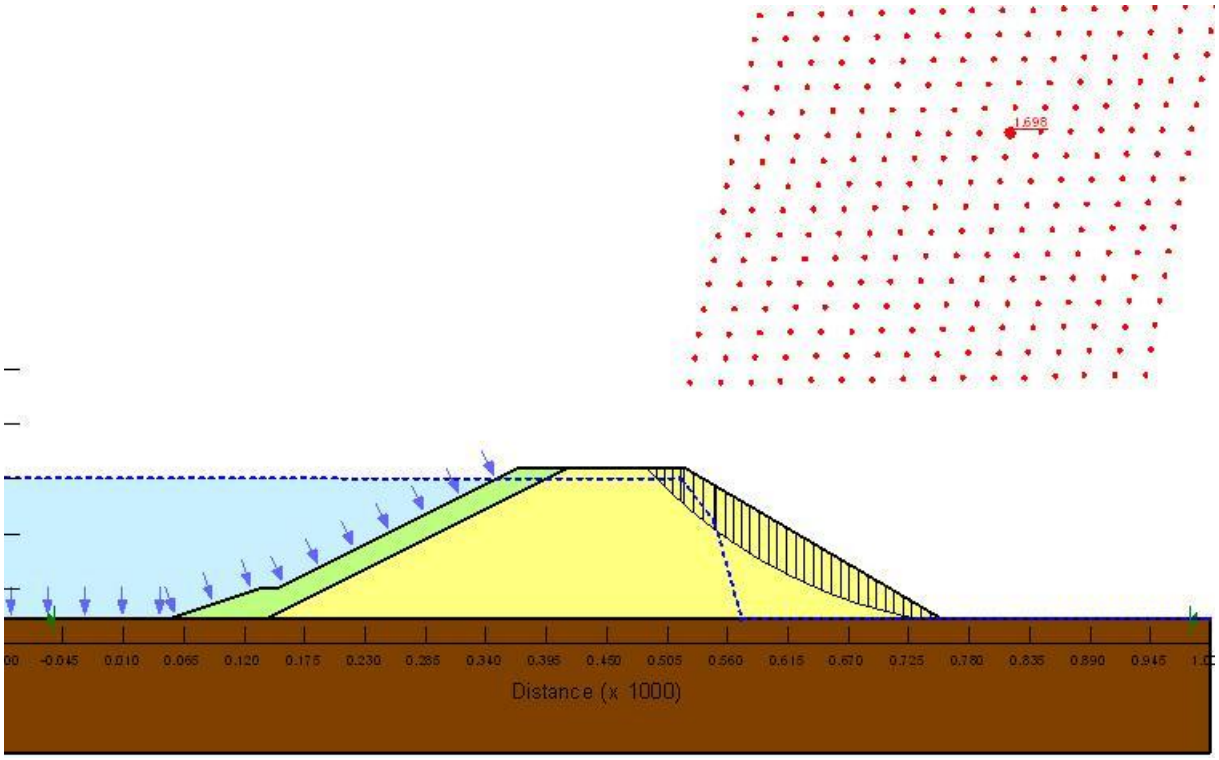

Figure 7.5 : Stage 1 critical slip circle – Normal water level – Downstream (SF=1.7)

The plastic deformation causes by an earthquake are evaluated thanks to the Swaisgood formula and are presented in the next table.

Earthquake	MCE
Crest settlement due to the earthquake (Swaisgood) (m)	1.10

Table 22: Stage 1 dam crest settlement during earthquake - Swaisgood formula

The yield acceleration that leads to a safety factor of 1, is 0.24g, ie a PGA of 0.36g. The critical slip circles on the upstream and downstream slopes are presented in the next figure.

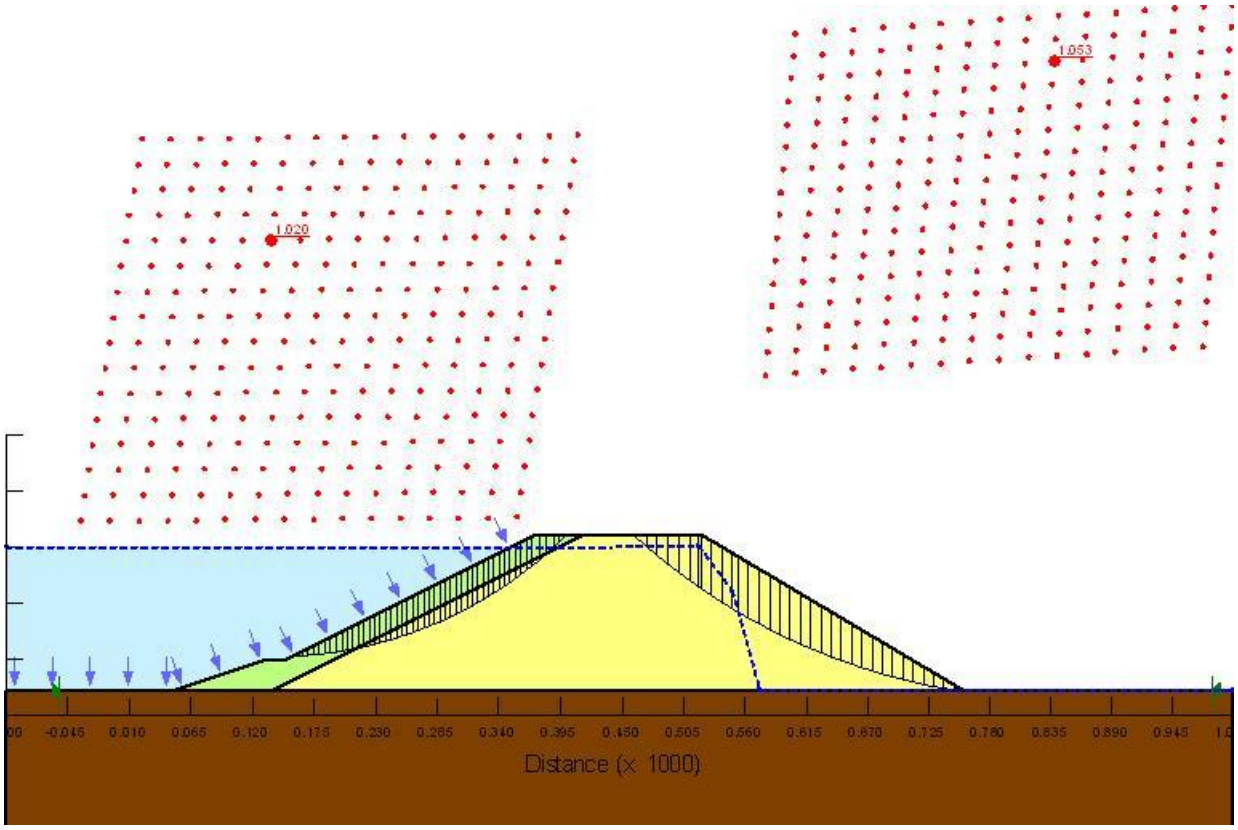

Figure 7.6 : Critical slip surface - yield acceleration of Stage 1 dam

7.5 Conclusion about Stage 1 dam stability

The Stage 1 dam upstream and downstream slopes are sufficient to ensure the stability of this construction phase.

As the cofferdam has the same material and upstream slope, softer dowsntream slope, and lower height than this Stage 1 configuration, it can be stated that the cofferdam stability is also secured.

8 CONCLUSION AND RECOMMENDATIONS

This report includes a brief review of the existing documentation made available by the Client to the Consultant, regarding stability analysis carried out by HPI. Then, based on the same typical dam cross section defined and justified by HPI, the Consultant carried out its own assessment. Conclusisons on this own assessment has been used to define Consultant own typical dam cross section.

The Rogun dam stability is ruled by the seismic load case. During MCE (Maximum Credible Earthquake), large irreversible deformation will occur: crest settlement and horizontal shear movement. Therefore, the analysis performed by the Consultant aims mainly at assessing the permanent displacements likely to occur during an extreme earthquake (MCE).

The study shows that the range of permanent displacement is 2-9 m horizontally and 1.5-6 m vertically.

The analysis also shows that during earthquake for all sections, the upper 50 m of the dam are the most critical in terms of acceleration and shear strain.

Based on those results the Consultant considers the following design features:

- Dam slopes should be kept as designed by HPI: 2H/1V downstream and 2.4H/1V upstream above the large berm level and 2H/1V below. Indeed, these slopes have been found sufficient to ensure the stability of the dam.

- Given the range of horizontal displacement found, filters and transitions thickness should be at least 10 m to ensure its continuity even in the case of a large earthquake.

- The freeboard should be at least 6 m to accommodate the settlement found likely to occur during a large earthquake to avoid dam overtopping.

- Special care should be given to the upper part of the dam (top 50 m): to limit mass sliding the Consultant prefers to set material such as rockfill that have a higher friction angle than the alluvium.

Three different cross sections of the dam have been studied: one in the river bed, one in the right bank and one on the left bank. The corresponding dam height ranges from 160 m to 335 m. This allows studying the sensitivity of the results with respect to the dam height. It can be seen that even if the dynamic behavior is slightly different from one dam height to another, the overall permanent displacement are in the same range of magnitude.

Therefore it is considered that, for alternatives comparison purposes, the same conclusions and recommendations are to be applied to the three dam alternatives and are used to derive the corresponding typical dam cross section.

Provided that the design features stated above are introduced in the various dam alternatives, the safety of the Rogun dam is ensured under static and seismic conditions.

Additional design measures, such as strengthening devices, are not necessary at this stage. However in further stages of the Project development, with the results of the three-dimensional seismic behavior analysis, such specific features shall be analyzed again. It should be outlined also that such reinforcement was not finally retained by HPI for Rogun, after the results of the more detailed calculations they performed.

Further study and optimization should be performed at later stages to determine precisely the dam behavior under the various loads, taking into account:

- The 3D geometry of the dam including the S-shaped valley and the very steep banks that tend to create arch effect and stress transfer to the banks;

- The elasto-plastic non-linear behavior of the material by using the advanced cyclic model such as hardening small strain model. It is worth noting that using the elasto-plastic non-linear analysis determines directly the permanent displacement as well as the excess pore pressure generating during the earthquake in the core.

APPENDIX 1 –ELASTIC ANLAYSIS

Natural frequency calculation for section 2-1.

Eigenvalue Analysis				Modal Mass participation (%)			
Mode No	Frequency	Frequency	Period	TRAN-X		TRAN-Y	
	(rad/sec)	(cycle/sec)	(sec)	MASS(%)	SUM(%)	MASS(%)	SUM(%)
1	5.16	0.82	1.22	58.93	58.93	0.03	0.03
2	7.64	1.22	0.82	0.01	58.94	26.31	26.34
3	8.61	1.37	0.73	3.72	62.66	1.93	28.28
4	9.49	1.51	0.66	0.01	62.67	1.42	29.7
5	10.37	1.65	0.61	15.94	78.61	0	29.7
6	11.73	1.87	0.54	0.02	78.63	16.56	46.26
7	12.28	1.96	0.51	0.16	78.79	4.47	50.73
8	12.76	2.03	0.49	0.17	78.97	0.2	50.93
9	14.24	2.27	0.44	0.3	79.27	3.52	54.44
10	14.54	2.31	0.43	1.61	80.88	2.75	57.19
11	15.40	2.45	0.41	0.07	80.95	2.32	59.52
12	15.71	2.50	0.40	0.06	81.01	0.06	59.58
13	16.28	2.59	0.39	0.82	81.83	5.27	64.85
14	16.75	2.67	0.38	3	84.84	1.33	66.18
15	17.61	2.80	0.36	0.29	85.12	0.46	66.64
16	17.79	2.83	0.35	0.43	85.56	1.08	67.71
17	18.05	2.87	0.35	0.28	85.84	0.24	67.96
18	18.44	2.93	0.34	0.47	86.3	0.02	67.98

19	18.88	3.01	0.33	0.17	86.48	0.08	68.06
20	19.66	3.13	0.32	1	87.48	0.06	68.13
21	20.03	3.19	0.31	0.44	87.92	0.13	68.25
22	20.42	3.25	0.31	0	87.92	4.76	73.02
23	20.72	3.30	0.30	0.19	88.11	0.57	73.59
24	21.36	3.40	0.29	0.06	88.17	2.5	76.09
25	21.53	3.43	0.29	0.17	88.33	0.15	76.23
26	22.16	3.53	0.28	0.12	88.45	0.04	76.27
27	22.71	3.61	0.28	0.09	88.54	1.29	77.56
28	22.88	3.64	0.27	0.96	89.5	0.55	78.11
29	23.55	3.75	0.27	0.04	89.55	0.01	78.12
30	23.76	3.78	0.26	0.54	90.09	0	78.12

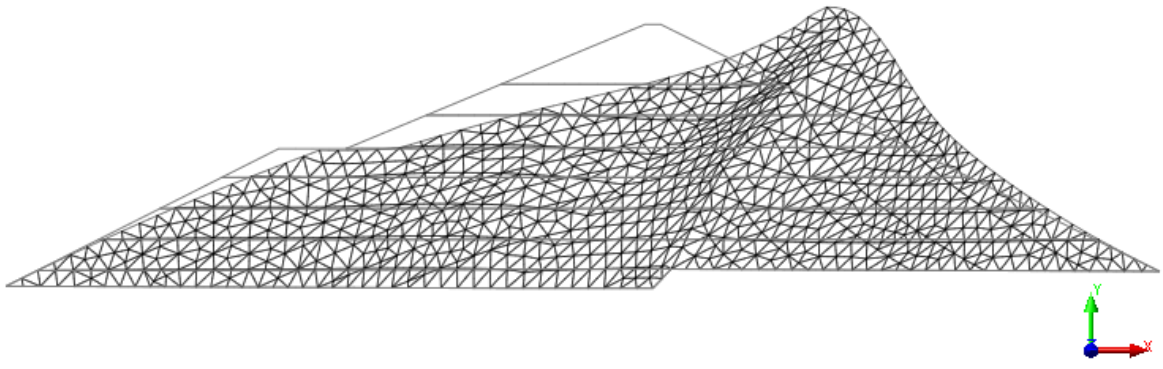

[UNIT] kN , m
[DATA] EIGN : Eigenvalues , DXYZ(V) , MODE 1: f(0.821722)

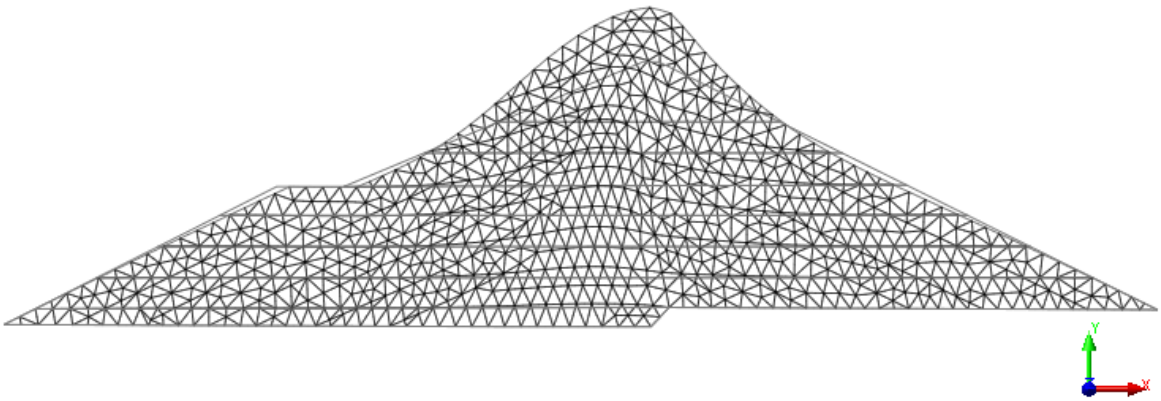

[UNIT] kN , m
[DATA] EIGN : Eigenvalues , DXYZ(V) , MODE 2: f(1.21642)

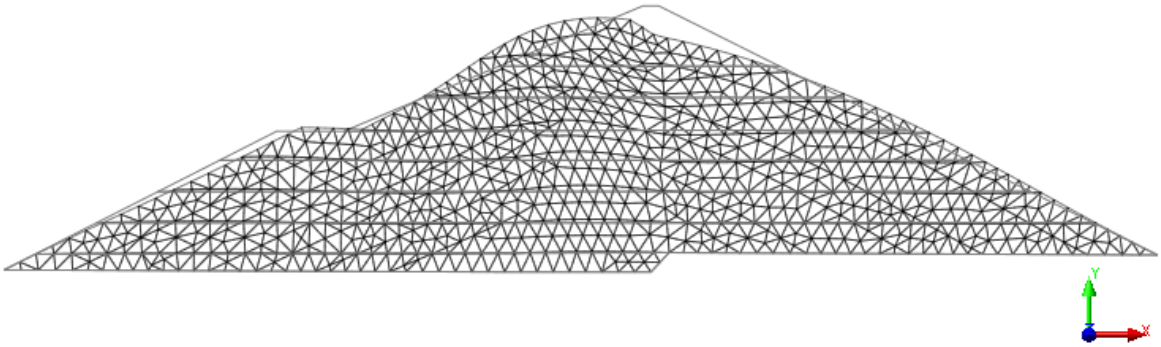

[UNIT] kN , m
[DATA] EIGN : Eigenvalues , DXYZ(V) , MODE 5: f(1.65037)

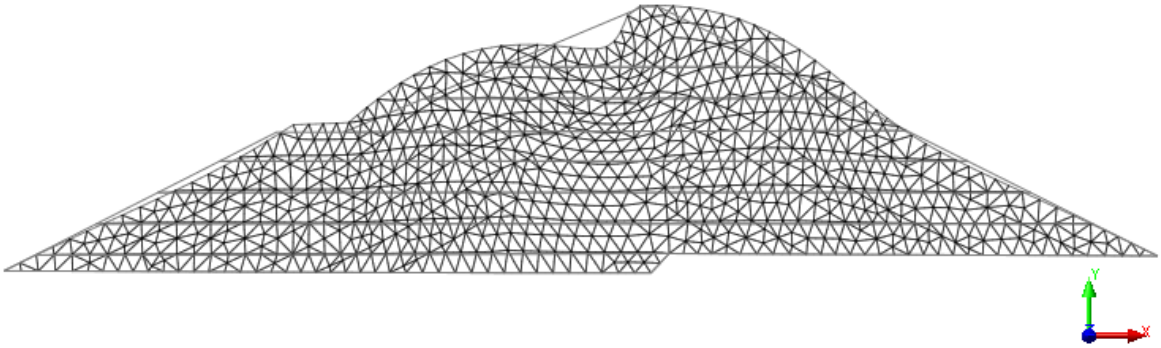

[UNIT] kN , m
[DATA] EIGN : Eigenvalues , DXYZ(V) , MODE 6: f(1.86667)

Natural frequency calculation for section 2-2.

Mode No	Frequency	Frequency	Period	TRAN-X		TRAN-Y	
	(rad/sec)	(cycle/sec)	(sec)	MASS(%)	SUM(%)	MASS(%)	SUM(%)
1	5.79	0.92	1.09	59.58	59.58	0.04	0.04
2	8.14	1.30	0.77	0.15	59.73	36.66	36.7
3	9.43	1.50	0.67	2.99	62.73	0.05	36.76
4	10.36	1.65	0.61	0.26	62.99	4.87	41.63
5	12.12	1.93	0.52	10.24	73.22	2.4	44.03
6	12.82	2.04	0.49	1.28	74.5	17.89	61.91
7	14.51	2.31	0.43	0.01	74.5	0	61.92
8	15.28	2.43	0.41	0.05	74.55	0	61.92
9	16.41	2.61	0.38	0.51	75.06	0.11	62.03
10	16.95	2.70	0.37	2.59	77.65	2.4	64.42
11	18.06	2.87	0.35	1.64	79.29	2.46	66.89
12	18.57	2.95	0.34	1.52	80.8	0.27	67.16
13	19.01	3.03	0.33	0	80.8	1.58	68.75
14	19.75	3.14	0.32	0.14	80.94	0.06	68.8
15	20.72	3.30	0.30	0.12	81.06	1.18	69.99
16	21.05	3.35	0.30	0.12	81.18	0.01	69.99
17	21.68	3.45	0.29	1.15	82.33	1.3	71.29
18	22.67	3.61	0.28	0.88	83.21	0.06	71.35
19	23.06	3.67	0.27	0.55	83.76	0.51	71.86
20	23.58	3.75	0.27	0	83.77	1.53	73.39
21	24.01	3.82	0.26	0.59	84.36	1.46	74.86
22	25.19	4.01	0.25	0.19	84.54	1.53	76.39
23	25.31	4.03	0.25	0.01	84.55	0.11	76.49
24	25.82	4.11	0.24	1.02	85.57	0.04	76.53
25	26.12	4.16	0.24	0.04	85.61	0.25	76.78
26	26.79	4.26	0.23	0.2	85.81	0.01	76.8
27	27.53	4.38	0.23	0.2	86.01	0.44	77.24
28	27.82	4.43	0.23	0.01	86.01	0.01	77.25
29	28.37	4.52	0.22	0	86.02	0.78	78.02
30	28.62	4.55	0.22	0.01	86.02	0	78.02

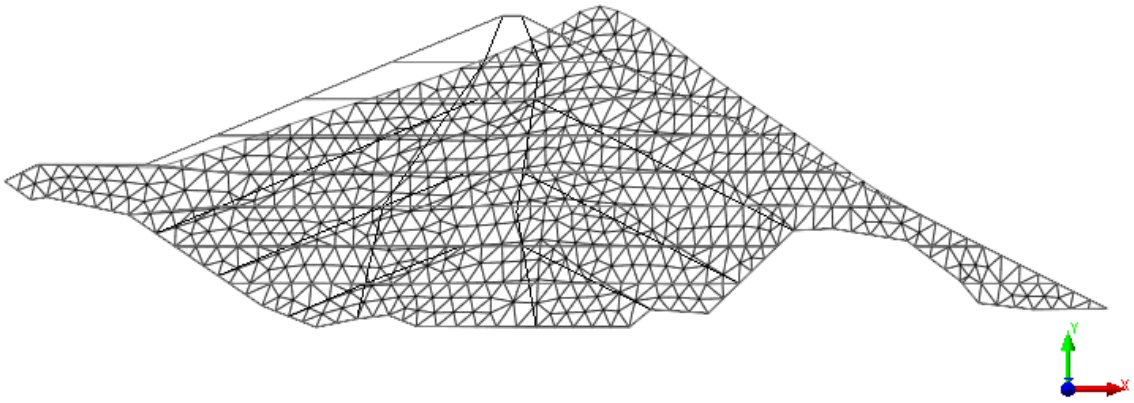

[UNIT] kN , m
[DATA] EIGN : Natural frequencies , DXYZ(V) , MODE 1: f(0.92084)

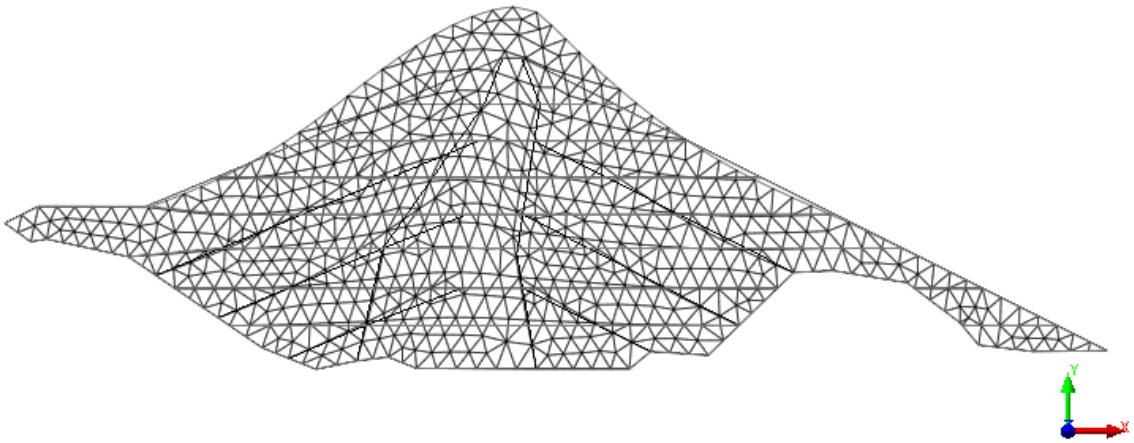

[UNIT] kN , m
[DATA] EIGN : Natural frequencies , DXYZ(V) , MODE 2: f(1.2961)

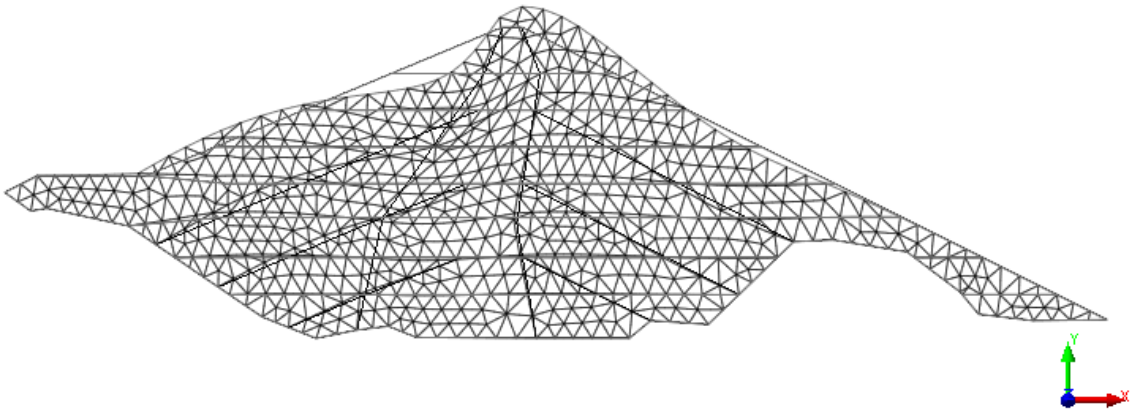

[UNIT] kN , m
[DATA] EIGN : Natural frequencies , DXYZ(V) , MODE 5: f(1.92902)

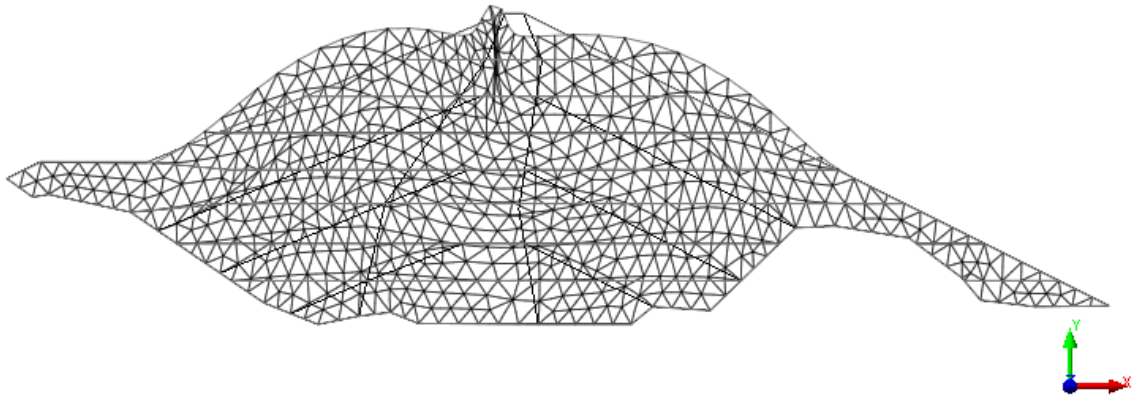

[UNIT] kN , m
[DATA] EIGN : Natural frequencies , DXYZ(V) , MODE 6: f(2.03966)

Natural frequency calculation for section 2-3.

Mode No	Frequency	Frequency	Period	TRAN-X		TRAN-Y	
	(rad/sec)	(cycle/sec)	(sec)	MASS(%)	SUM(%)	MASS(%)	SUM(%)
1	8.01	1.27	0.78	36.19	36.19	0.15	0.15
2	11.20	1.78	0.56	0.03	36.22	15.22	15.37
3	12.50	1.99	0.50	24.15	60.37	0.33	15.71
4	12.54	2.00	0.50	5.38	65.74	0.76	16.46
5	14.25	2.27	0.44	1.44	67.18	2.37	18.83
6	15.38	2.45	0.41	0.54	67.72	0	18.83
7	16.24	2.58	0.39	0	67.72	0.13	18.97
8	17.49	2.78	0.36	0.31	68.03	17.06	36.03
9	17.94	2.85	0.35	0.75	68.78	0.05	36.08
10	18.20	2.90	0.35	3.52	72.29	13.65	49.74
11	18.40	2.93	0.34	1.37	73.66	5.95	55.69
12	18.71	2.98	0.34	1.44	75.11	0.04	55.73
13	18.99	3.02	0.33	0.25	75.35	1.11	56.84
14	19.54	3.11	0.32	0.03	75.38	3.13	59.97
15	20.46	3.26	0.31	0	75.38	1.56	61.54
16	21.30	3.39	0.30	0.72	76.1	0	61.54
17	21.65	3.45	0.29	1.05	77.15	3.23	64.77
18	22.24	3.54	0.28	0	77.15	4.72	69.49
19	23.13	3.68	0.27	0.32	77.48	0.38	69.86
20	23.30	3.71	0.27	0.13	77.61	2.06	71.92
21	23.88	3.80	0.26	0.7	78.3	0.13	72.04
22	24.50	3.90	0.26	0.08	78.39	1.98	74.02
23	25.12	4.00	0.25	0.32	78.71	0.45	74.48
24	26.01	4.14	0.24	1.01	79.72	0.09	74.56
25	26.29	4.18	0.24	0.07	79.79	1.27	75.83
26	26.57	4.23	0.24	0.77	80.56	0.35	76.18
27	27.64	4.40	0.23	0	80.56	0.09	76.27
28	27.80	4.42	0.23	0.66	81.22	0	76.27
29	28.20	4.49	0.22	1.18	82.41	0.19	76.46
30	28.77	4.58	0.22	0.7	83.11	0.33	76.79

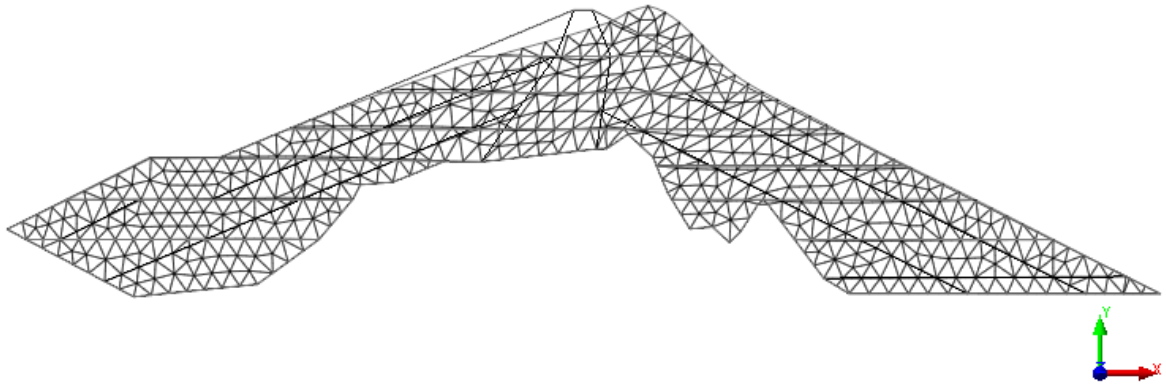

[UNIT] kN , m
[DATA] EIGN : Natural frequencies , DXYZ(V) , MODE 1: f(1.27495)

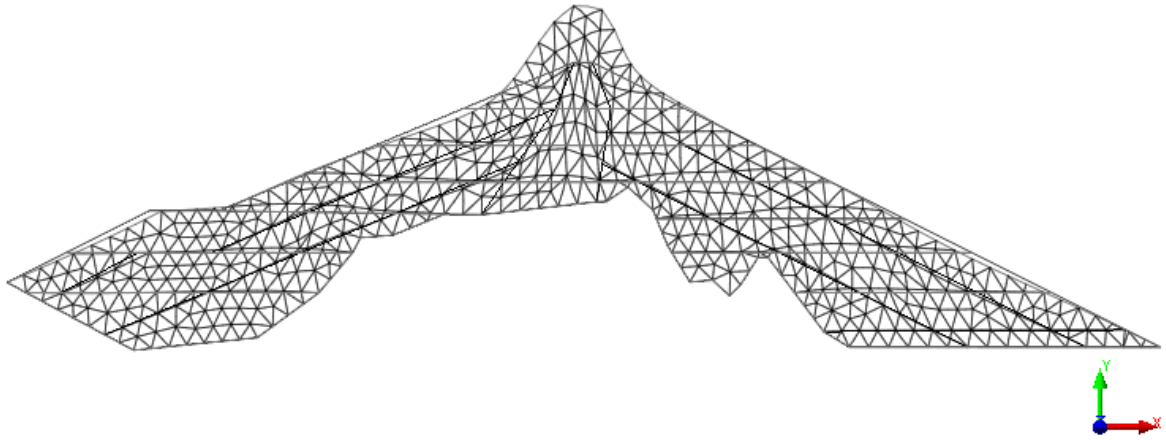

[UNIT] kN , m
[DATA] EIGN : Natural frequencies , DXYZ(V) , MODE 2: f(1.78175)

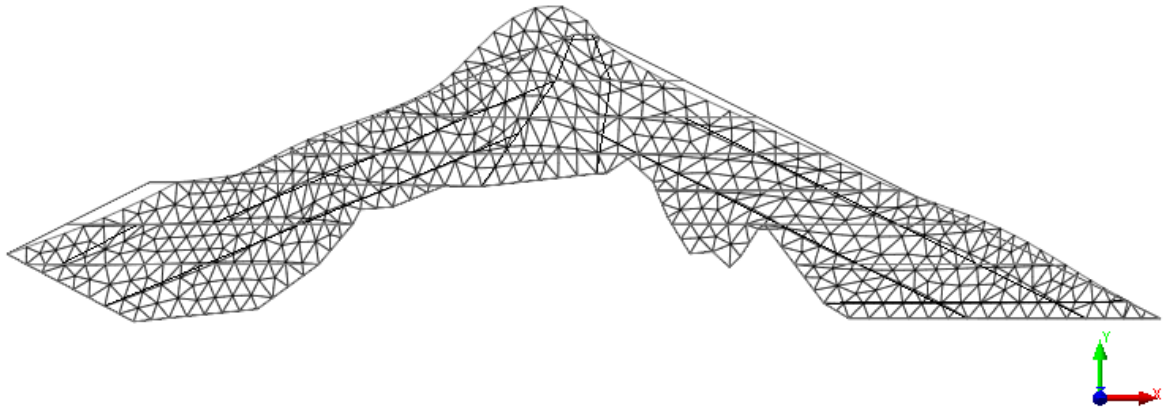

[UNIT] kN , m
[DATA] EIGN : Natural frequencies , DXYZ(V) , MODE 3: f(1.98954)

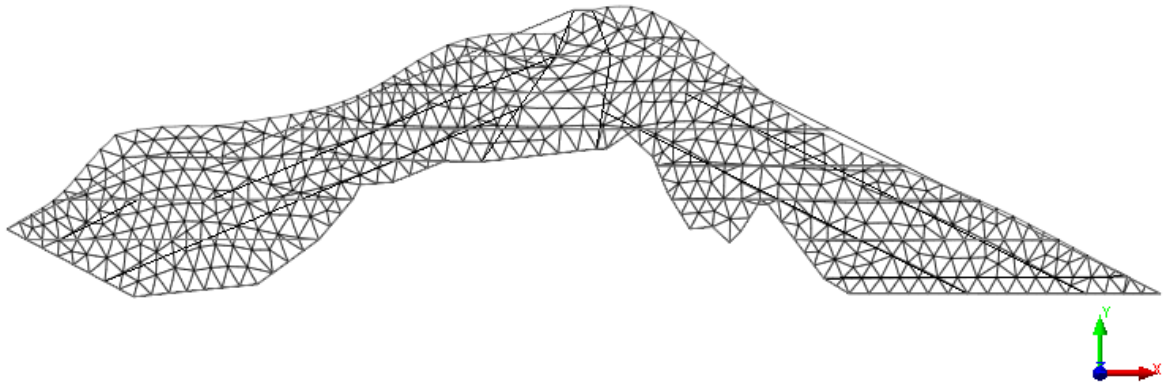

[UNIT] kN , m
[DATA] EIGN : Natural frequencies , DXYZ(V) , MODE 8: f(2.78327)

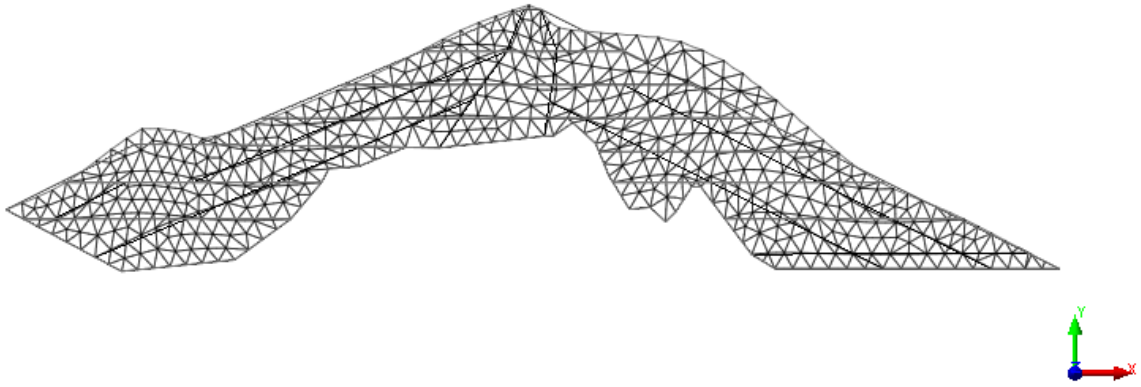

[UNIT] kN , m
[DATA] EIGN : Natural frequencies , DXYZ(V) , MODE 10: f(2.89726)